DEPARTMENT OF TRANSPORTATION

Dowel – Concrete Interface Performance Validation in Concrete Rehabilitations

Bernard Izevbekhai, Principal Investigator
Office of Materials and Roads Research
Minnesota Department of Transportation

October 2024

Research Report
Final Report 2024-24

To get this document in an alternative format or language, please call 651-366-4720 (711 or 1-800-627-3529 for MN Relay). You can also email your request to ADArequest.dot@state.mn.us. Please make your request at least two weeks before you need the document.

Technical Report Documentation Page

1. Report No.	2.	3. Recipients Accession No.	
MN 2024-24			
4. Title and Subtitle Dowel – Concrete Interface Performance Validation in Concrete Rehabilitations		5. Report Date September 2024 6. .	
7. Author(s) Bernard Izevbekhai, Ceren Aydin, Maria Masten, Gordon Bruhn		8. Performing Organization Report No.	
9. Performing Organization Name and Address Office of Materials and Roads Research Minnesota Department of Transportation 1400 Gervais Avenue Maplewood, MN 55109		10. Project/Task/Work Unit No. 11. Contract (C) or Grant (G) No.	
12. Sponsoring Organization Name and Address Minnesota Department of Transportation Research Services & Library 395 John Ireland Boulevard, MS 330 St. Paul, Minnesota 55155-1899		13. Type of Report and Period Covered Final Report 14. Sponsoring Agency Code	
15. Supplementary Notes http://mdl.mndot.gov/			

16. Abstract (Limit: 250 words)

The Minnesota Department of Transportation (MnDOT) investigated the use of dowels with various anchoring methods and their effects on pavement performance. In a previous study, the characteristics of various epoxy and grout anchorage systems at the interface between new construction and existing concrete were studied using cut-out slabs brought into the Minnesota Road Research Facility (MnROAD). This investigation seeks to validate the findings of that study. Twelve different anchoring materials and methods were studied and compared to a control using no grout. This study did not examine the effects of a reduced number of dowels across a lane but rather looked at only the anchorage materials and methods. This experiment was performed on westbound lanes of Interstate 94, adjacent to the MnROAD test track. The field experimentation and monitoring involved core samples and measured ride quality, International Roughness Index (IRI), and Falling Weight Deflectometer (FWD) load transfer and fault measurement. These results supplemented the findings from the previous in-house performance categorization experiment. The control experiment, conducted without any grout or epoxy, initially displayed a notably low Load Transfer Efficiency (LTE). However, over time, there was a gradual improvement, leading to a more consistent LTE, attributed to the deployment of non-mechanical load transfer. Based on the slab thickness, the 1.25-inch dowel did not indicate any statistically significant LTE or other performance improvements over the 1-inch dowel within the anchorage types examined. Overall, the Epoxy Experimental 1 performed best while the un-grouted and unrepaired cells had the lowest performance. Moreover, no material clearly indicated characteristically low performance.

17. Document Analysis/Descriptors	18. Availability Statement		
Dowels (Fasteners), Anchorages, Dowel bar retrofit, Epoxy coatings	No restrictions. Document available from: National Technical Information Services, Alexandria, Virginia 22312		
19. Security Class (this report)	20. Security Class (this page)	21. No. of Pages	22. Price
Unclassified	Unclassified	53	

Dowel – Concrete Interface Performance Validation in Concrete Rehabilitations

Final Report

Prepared by:

Bernard Izevbekhai, P.E., Ph.D.
Ceren Aydin, Ph.D.
Maria Masten, P.E.
Gordon Bruhn
Office of Materials and Road Research
Minnesota Department of Transportation

October 2024

Published by:

Minnesota Department of Transportation
Office of Research & Innovation
395 John Ireland Boulevard, MS 330
St. Paul, Minnesota 55155-1899

Acknowledgements

Support variously rendered by Jeffrey Brunner, (Research Director) Curt Turgeon (Pavement Manager), and Glenn Engstrom (Office Director) in the Minnesota Department of Transportation (MnDOT) Office of Materials and Road Research were invaluable. The authors are also indebted to MnROAD Operations staff including Steven C. Olson for test cell monitoring and response to data requests for this research project. Authors acknowledge the Technical Advisory Panel (TAP) made up of Benjamin Worel (MnROAD Operations Engineer) Tom Burnham (Senior Pavement Research Engineer) and Eddie Johnson (Research Projects Engineer) in the MnDOT Office of Materials and Road Research who provided useful reviews and helpful feedback.

Table of Contents

List of Figures

List of Tables

List of Abbreviations

IRI: International Roughness Index
FWD**:** Falling Weight Deflectometer
LTE: Load Transfer Efficiency
MnDOT: Minnesota Department of Transportation
MnROAD: Minnesota Road Research Facility
LWP: Left Wheel Path
RWP: Right Wheel Path

Executive Summary

In regular full-depth concrete rehabilitation projects, repair limits are tied to saw-cut ends by grout or epoxy-anchored dowels. Adequate anchorage of the dowels to the existing concrete ensures compatibility and should consequently forestall subsidence and other premature distresses.

However, numerous occurrences of subsidence at some of these concrete repair locations in some concrete rehabilitation projects posed a challenge to reexamine the suitable number of dowels across each 12-ft wide panel and the various anchorage materials and mechanisms used. This research report examines the characteristics of various epoxy and grout anchorage systems at the interface between new construction and existing concrete.

A previously performed indoor experiment examined 12 different materials and procedures as well as a control experiment. That report is being published simultaneously with this report. This field experiment continued the previous effort using 13 test cells each consisting of 11 dowels across each joint at one-foot intervals. Researchers did not examine the effect of a reduced number of dowels per cross-section within the scope of the study. The experiment identified the tube grout method as the best anchorage material based on ride quality, International Roughness Index, (IRI), and Load Transfer Efficiency (LTE). The control experiment, conducted without any grout or epoxy, initially displayed a notably low LTE. However, over time, there was a gradual improvement, leading to a more consistent LTE, attributed to the deployment of non-mechanical load transfer (base and aggregate interlock) following the load repetitions. The 1.25-inch dowel did not indicate any statistically significant LTE improvement over the 1-inch dowel within the anchorage types examined.

Chapter 1 discusses the background of the efforts performed within the scope of this report. A previous experiment, performed in-house, involved a concrete slab that was used to test all methods of dowel bonding. The current report is a continuation of the previous experiment's efforts, wherein the methods examined previously were applied in a deployment study on test cells situated adjacent to the Minnesota Road Research Facility (MnROAD).

Chapter 2 examines the design process of the experiment. The setup of the cells and their given fixes are described and the differences between the lanes are established. The methods used to study the results of the experiment are discussed, including the Falling Weight Deflectometer (FWD), IRI, and visual analysis.

In Chapter 3 the results are examined and discussed, including IRI measurements derived from both the initial two measurements and subsequent ones up to 2018. Additionally, the chapter incorporates results from FWD tests and visual inspections.

Chapter 4 delves into the conclusions and recommendations. The research, based on pavement smoothness, load transfer, and visuals, showed that the epoxy and grout-filled cells performed better than those without grout or epoxy, and much better than the unrepaired portion. The Epoxy Experimental 1 appeared to be the best-performing material. The majority of the time, the 1-inch

diameter demonstrated better performance than the 1.25-inch diameter dowel in this experiment. The unrepaired sub cell showed a plane of delamination tangential to the dowel. This plane appeared to be a logical stress relief mechanism in reaction to the bearing stresses occurring in a distressed anchorage system. It emerged that socketing would continue to occur when there was no plane of delamination. The factor that selectively results in socketing versus plane of delamination is a fracture-mechanics issue that is beyond the level of this report.

Chapter 1: Introduction

1.1 Background

Sustainable approaches to pavement construction consist of concrete overlays including unbonded overlays, whitetopping of flexible pavements, and concrete rehabilitation. The rehabilitation of concrete is ramified into minor rehabilitation and major rehabilitation. In minor rehabilitations, a few partial-depth repairs and full-depth repairs are performed per lane-mile of the project with an emphasis on the interval between them. In major rehabilitations, there are typically full-depth repairs, dowel-bar retrofits, and a few partial-depth repairs, which occur at short intervals within the control section or project area [1]. In all full-depth repairs, it is always necessary to tie the new concrete material to the existing concrete. In practice, this is achieved by gang-drilling into the existing concrete, placing dowels, and grouting or epoxying the holes drilled at a prescribed spacing such that a specified number of dowels across the panel are inserted and anchored with acceptable anchorage materials [2]. Two aspects of the challenge of dowel bar anchorage has been the sufficiency of the number of dowels at the end of a full-depth concrete repair and choosing an adequate interface bond material or installation process that maximizes the performance of the repairs. The traditional method of rehabilitation typically entails gang-drilling and then inserting dowels at the one-foot center-to-center spacing and anchoring with epoxy or grout. In typical MnDOT rehabilitation projects in the past, there were 12 dowels installed across the lane. Sometime in 2011, 11 dowels across the lane were tried by the contractors. Subsequently, this was reduced to seven and later to six dowels with three on each wheel path. There was no consensus as to the sufficiency of the six dowels, particularly as a finite element or similar analysis was not conducted. During the period, widespread subsidence was observed. It was also suggested that the methods of anchorage used for compatibility between the existing concrete and the repaired portion may have been defective. It became necessary to ascertain the evenness and uniformity of application of grout or epoxy around the annular space between the drilled hole and the dowel and to determine using acoustic impedance which materials and processes were defective and which were marginal or suitable. There was a consideration regarding whether the primary issue lied in the challenge of selecting the appropriate grout or epoxy.

Although sinking supports are not commonly mentioned, a true and beneficial design process will use some form of perturbation to ascertain induced moments and design against them. It is the design against subsidence and the process that ensures uniform support that assures the pavement engineer that moments need not be considered in the design. Very little has been specifically done in relating this phenomenon to jointed plain concrete pavements with or without dowels. Sinking support moment of a propped cantilever of displacement (δ) can be expressed as shown in Figure 1.1.

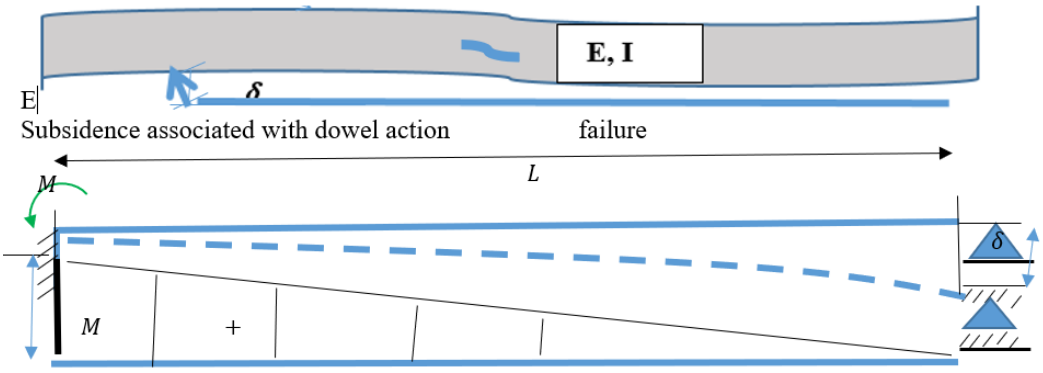

Figure 1.1: Rigid panel with sinking support

Considering the panel in Figure 1.1, it can be shown that:

$$M = \frac{3EI\delta}{L^2} \qquad (1)$$

Where E is Elastic modulus, I is moment of Inertia, L is panel length, M is induced moment and the quantity δ is the sinking support displacement that is inducing the moment.

It can be also shown that:

$$R = \left[\frac{Eh^3}{12(1-\mu^2)k}\right]^{0.25} \qquad (2)$$

Where R is the radius of relative stiffness, B is the panel width, K is modulus of subgrade (base) reaction, the quantity μ is Poisson's ratio, the quantity h id the panel thickness.

Combining equations (1) and (2) it can be shown that

$$M = \frac{3bk(1-\mu^2)\delta R^4}{h^3 L^2} \qquad (3)$$

As we thin out pavements one set back is that there is an increase in induced moments when all things are held constant in comparison to thicker pavements. Sinking support moments are non-trivial and should not be neglected in pavements.

This experiment was a deployment of the preliminary in-house experiment into an actual rehabilitation project on Westbound Interstate 94 in 2013, adjacent to the MnROAD test-track lanes. Actual rehabilitation of the 27-foot panels included real-time panel anchorage by gang-drilling and using the same factorial of epoxies and grouts that were used in the pole barn experiment. A data collection scheme including measurement of International Roughness index (IRI) and the use of the Falling Weight deflectometer (FWD)for load transfer and layer moduli was initiated. This work plan identified the analytic work requested by the MnDOT Concrete Engineering Unit to facilitate the performance trend in the subsections of the dowel bar anchorage experiment.

1.2 Synthesis

Gang-drilling is used in “full-depth” repairs. During these repairs, dowel bars must be placed in the transverse joints at the limits of cuts and repairs. It is essential to properly clean the dowel holes prior to installing new dowels. In this project, the dowel holes were cleaned by inserting a compressed air nozzle into the back of the hole. The compressed air removed debris present from the drilling process. If the debris was not significantly removed, it prevented the adhesive material from properly bonding to the concrete. When using the air compressor, it was important to occasionally check the air for oil and moisture contamination. If contaminated, correct bonding within the drilled holes would be inhibited.

Following drilling dowel holes, the anchoring material was injected into the back of each hole using a long nozzle. This ensured that the anchoring material flowed forward along the entire dowel embedment length during insertion, decreasing the likelihood of leaving voids between the dowel and the concrete. It was shown that ready-made epoxy cartridges supplied enough material for one to two holes. It should be noted that a more cost-effective method for large projects, a pressurized injection system from bulk epoxy containers is recommended. The injection wand on the installation unit should contain an auger-type mixing spindle to mix a two-part epoxy. However, when using non-shrink cementitious grouts, a caulk-gun type tool is preferable.

The injected anchoring material can occasionally flow out while inserting the dowels. A plastic grout-retention disk is occasionally used to provide a barrier that prevents the escape of the anchoring epoxy or grout. When there has been a sufficient amount of material injected, some anchoring material should be visible from the sides of the disk after installation. If no anchoring materials are seen, there may not be enough in the hole. If retention disks are not available, some extra grout should be placed around the dowel. While not ideal, this is preferable to leaving a void. Ideally, anchoring materials will remain in the hole without the use of a retention disk. If it is difficult to control the loss of material, it may be necessary to adjust the mix. Small batches should be mixed for non-shrink, cementitious material because these materials stiffen with time after mixing, changing their installation properties.

1.3 Objective

The traditional method of full-depth rehabilitation in Minnesota entailed gang-drilling holes at one-foot center-to-center spacing, resulting in 12 dowels across the 12-foot cross-section. This was changed in a few projects in 2011 and 2012 to 11 dowels across to minimize redundancy and match changes to mainline concrete dowel practices. Following this change, widespread subsidence was observed on several projects. Besides dowel spacing, it was also suggested that the methods of anchorage that were critical to the compatibility between the existing concrete and the repaired portion may have been defective.

This experiment was limited to the examination of the anchorage at one-foot center-to-center across the lanes using the various grouting and epoxy products and processes. The experiment monitored the

test cells for immediate subsidence, semi-long-term subsidence, and performance trends. Since IRI and LTE were identified as proxies for performance trends, these were monitored seasonally.

A comprehensive experiment framework was deployed to compare the performance trends of the various grout and epoxy materials and processes but was limited in scope to exclude the determination of optimum dowel intervals. This experiment assumed that the prudent configuration of 11 dowels across the 12-ft lane was sufficient and proceeded to examine the adequacy of the various grouting and epoxying techniques with the 11-dowel cross-sectional configuration.

Chapter 2: Research Design

2.1 Design Summary

A deployment experiment was performed on the Old Westbound I-94 test track located adjacent to the MnROAD facility mainline in the Old Westbound lanes. The MnROAD mainline consists of a 3.5-mile stretch of Interstate Highway 94 consisting of a two-lane interstate roadway carrying “live” traffic. The third track, known as the Old Westbound, is the set of lanes to which traffic is diverted when the MnROAD mainline cells are being tested. This 3.5-mile-long segment consists of two 12-foot-wide lanes built with jointed reinforced concrete panels of 27-foot joint spacing.

The section was subdivided into a contiguous array of thirteen 81-foot sub cells, each with a unique grout/epoxy material and process, and with a driving and passing lane each, where the driving lane was diamond ground. The test cell establishment followed the same process used in traditional repairs. The steps identified in establishing and anchoring the dowels are shown in Figure 2.1 and Figure 2.2. While Figure 2.1 shows the steps (Steps 1 to 4) for the dowels interspersed with transient methods (three equally spaced dowels on each wheel path), practiced for a brief time by practitioners. In Step 1, the removal of the distressed portion of the pavement was performed. Once the distressed portion of the panel was removed the exposed existing slab was gang drilled at the slab mid depth. After drilling the dowel holes in the existing concrete slab, the holes were cleaned using an air compressor and a brush to ensure that the holes were free of all debris (Step 2). In Step 3, dowels were inserted along with or after proper epoxy or grout which was followed by pouring the slab concrete and reestablishing the joints where necessary days after inserting the dowels (Step 4) (Figure 2.1). Following the final step, diamond grinding, typically performed for concrete repairs, was carried out solely on the driving lane cells for the scope of this report. It's important to note that the transient method was linked to significant subsidence, thus rendering it short-lived. Figure 2.2 shows the traditional method with eleven equidistant dowels across lanes which followed the steps in Figure 2.1.

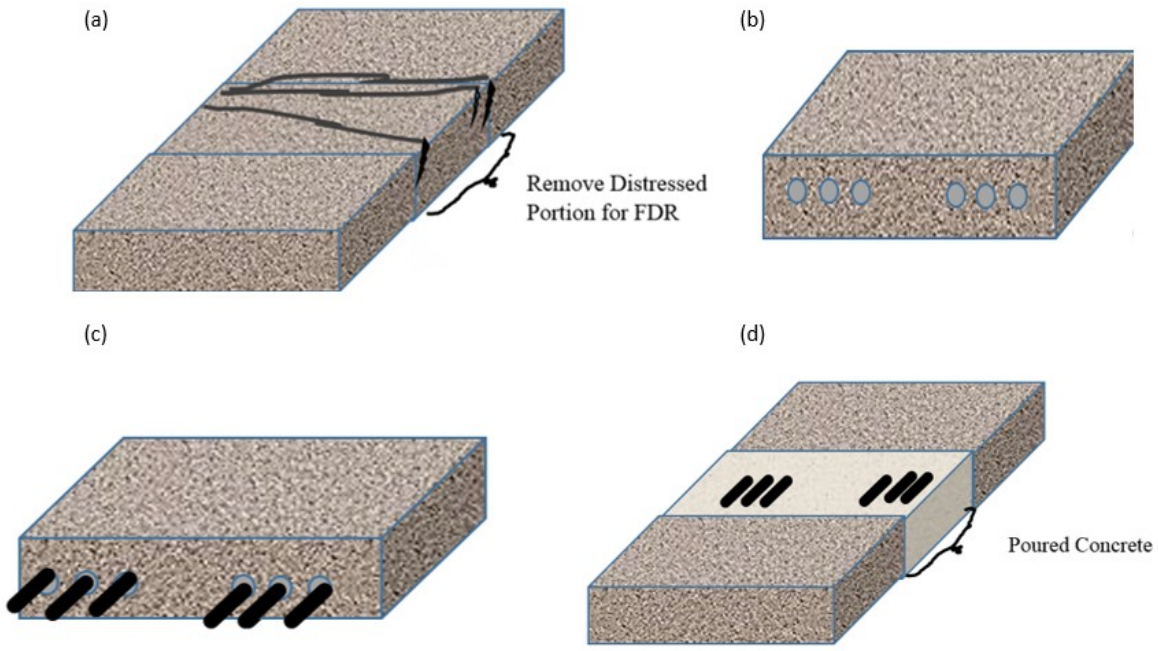

Figure 2.1 Transient method: (a) Step 1 - identify and remove slab portion, (b) Step 2 - gang drill existing slab, (c) Step 3 - insert dowel along with or after proper epoxy or grout, (d) Step 4 - pour the slab concrete and reestablish joints where necessary.

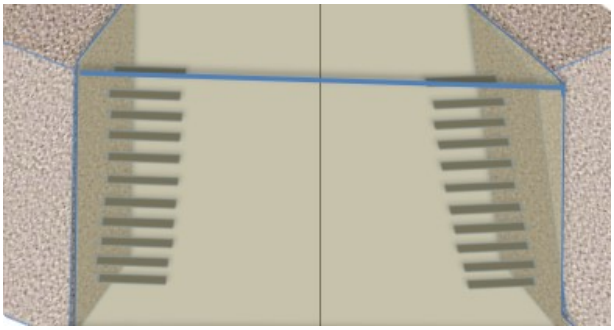

Figure 2.2 Traditional process with eleven dowels across.

The layout of the various sub cells is shown in Figure 2.3. There were a total of thirteen cells involved in this study, with six different dowel repair methods and processes analyzed, in addition to the control Sub Cell 982 experiencing no repairs. The purpose of Sub Cell 982 was to provide a reference for the test cells being repaired. Data collected from Sub Cell 982 highlighted the degree to which dowel repairs improved the function of the pavement. The implementation of the six different repair processes have been dispersed throughout the remaining twelve sub cells. There were two sub cells for every repair method, with each repair method evaluated by utilizing either 1" or 1.25" diameter dowel bars.

EAST

Sub Cell Number	970				971				972				973			
Length (ft)	13.5	27	27	13.5	13.5	27	27	13.5	13.5	27	27	13.5	13.5	27	27	13.5
Joint Number	1	★	2	★	3	1	★	2	★	3	1	★	2	★	3	1	★	2	★	3
Dowel Diameter (in)	1					1.25					1					1.25				
Grout/Epoxy	No Grout					No Grout					Grout: Bag Injected					Grout: Bag Injected				
Sub Cell Number	974				975				976				977			
Length (ft)	13.5	27	27	13.5	13.5	27	27	13.5	13.5	27	27	13.5	13.5	27	27	13.5
Joint Number	1	★	2	★	3	1	★	2	★	3	1	★	2	★	3	1	★	2	★	3
Dowel Diameter (in)	1					1.25					1					1.25				
Grout/Epoxy	Grout: Dip Method					Grout: Dip Method					Grout: Capsule Method					Grout: Capsule Method				
Sub Cell Number	978				979				980				981			
Length (ft)	13.5	27	27	13.5	13.5	27	27	13.5	13.5	27	27	13.5	13.5	27	27	13.5
Joint Number	1	★	2	★	3	1	★	2	★	3	1	★	2	★	3	1	★	2	★	3
Dowel Diameter (in)	1					1.25					1					1.25				
Grout/Epoxy	Epoxy Experimental 2					Epoxy Experimental 2					Epoxy Experimental 1					Epoxy Experimental 1				
Sub Cell Number	982															
Length (ft)	13.5	27	27	13.5												
Joint Number	1	★	2	★	3											
Dowel Diameter (in)	1															
Grout/Epoxy	Control															

WEST

★ FWD Points (26 per sub cell)
Diamond Grinding was performed for all the cells.
All repairs were full-depth joint repairs.

Figure 2.3 Test cells on the MnROAD Old Westbound test track evaluating epoxy/grout dowel system.

Figure 2.4 shows some of the anchorage processes.

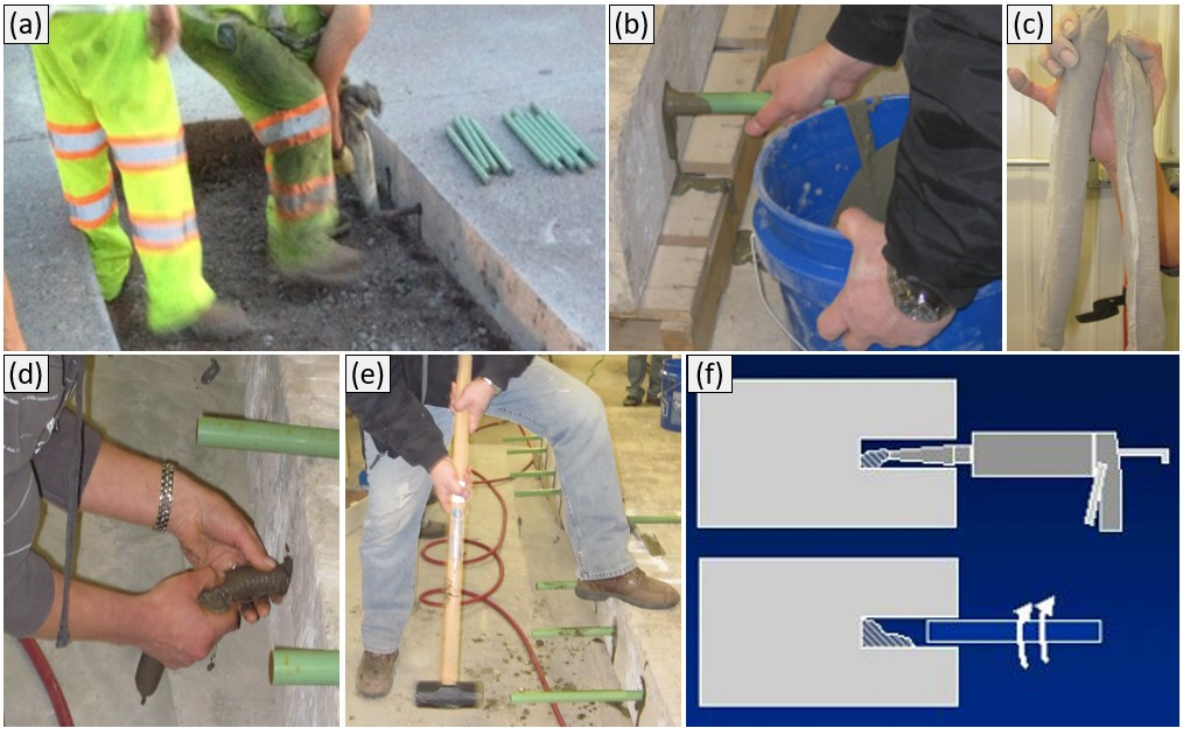

Figure 2.4 Anchorage processes: (a) full-depth repair with bar placement after drilling, (b) grout dowel bar injection, (c) saturated grout capsules, (d) pre-insertion of saturated grout capsule into pre-drilled hole, (e) sledge-hammer impact on dowels, (f) insertion of dowel bar into pre-drilled hole utilizing epoxy.

The repair methods were described strictly according to the adhesive material being used within the test sub cell. Sub Cells 970 and 971 consisted of the dowel repairs without a grout, meaning that the dowels were inserted with no adhesive material. The grout bag injected method was implemented in Sub Cells 972 and 973. The bag injection method consisted of applying the grout using a pastry-type bag within the drilled dowel hole. Another repair method investigated in this research was the grout dip method; deployed in Sub Cells 974 and 975. The grout dip method consisted of dipping the dowel bar into the mixed grout to a depth of the pre-drilled hole. Once the bar is properly coated in the grout, the dowel bar was inserted to the full depth of the hole as shown in Figure 2.4b. While inserting the dowel using the grout dip method, it was essential to twist the dowel one full revolution in order to evenly distribute the material around the entire dowel circumference. The final dowel repair method tested in this research utilized the grout capsule method; implemented in Sub Cells 976 and 977. This repair method utilized cementitious grout encapsulated in pre-measured grout packets consisting of water permeable wrapping, shown in Figure 2.4c. The grout capsule is saturated in water and then inserted into the pre-drilled hole Figure 2.4d. Immediately after inserting the grout capsule, the dowel bar was inserted and driven into the dowel hole using a hammering force Figure 2.4e. This option performed the best in the in-door experiment and was observed for validation in the deployment experiment. In addition to the grout repair methods previously described, two epoxy repair materials (Epoxy Experimental 1 and 2) were used within the scope of this research. Experimental Epoxy 1 (Sub Cells 980 and 981) refers to the weld low viscosity product and Experimental Epoxy 2 refers to another brand of epoxy used within the Sub Cells 978 and 979. The former was generally touted as a “weld”. Both epoxies analyzed in this research were installed using the same method. When utilizing epoxy for dowel installation, the anchoring epoxy should be injected into the hole for optimal effectiveness. This was completed using an injection wand that contains an auger-type mixing spindle that mixes the two-part epoxy. The dowel bar installation method for an epoxy involved twisting the dowel one full revolution during insertion to evenly distribute the material around the dowel’s circumference. The twist is substantial since it prevents grout remaining along the bottom of the bar which cause voids to form along the top of the bar. A schematic of this process is shown in Figure 2.4f.

IRI and LTE are the two primary pavement quantities that were assumed to be most affected by the dowel bar repairs. The lightweight inertial surface analyzer (LISA) and the FWD were the testing equipment used for the ride quality and LTE, respectively. The equipment were used to collect data on the sub cells for in-depth analysis, creating the potential for inferences to be drawn from the comparative performance of the various repair methods within the scope of the report.

The ride quality of pavement defines the comfort level experienced by drivers when riding on it. Ride quality was measured with the MnDOT lightweight profiler outfitted with an accelerometer on each side to measure IRI on each wheel path. IRI is the Average Rectified Value of the Slope Power Spectrum Density. A large IRI value corresponds to a road surface that has a significant amount of vertical acceleration of the quarter car suspension algorithm, making for a rougher ride experienced by drivers. At the time of testing, the LISA used at MnROAD consisted of two different laser technology apparatus’: ROLINE and TriODS. The TriODS system collects ride quality data using three-point lasers, whereas the

ROLINE system utilizes a line laser (Figure 2.5). The difference in values between the two systems (when small) is a quality assurance that the influence of texture is not unduly affecting IRI measurements.

Figure 2.5 Light weight profiler.

The FWD (Figure 2.6) measures load induced deflections, allowing for the determination of pavement layer moduli and the degree of load transfer across joints. Joint load transfer testing was performed by dropping the falling weight on one side of the joint and recording the subsequent deflections at the location of the weight's impact and the deflections on the other side of the joint, shown in Figure 2.6. The ratio of these two deflections was recorded as the load transfer efficiency (LTE) [3,4].

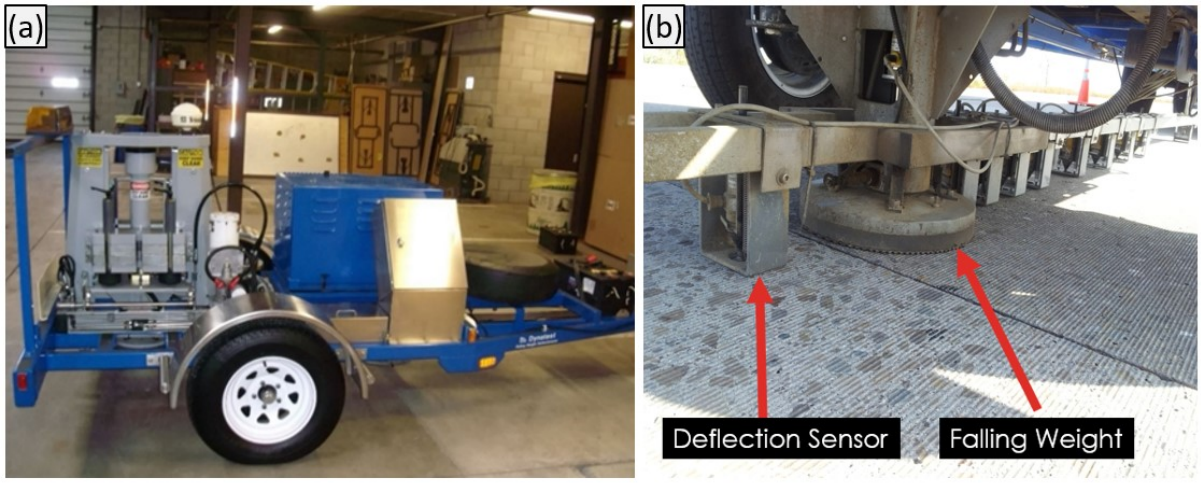

Figure 2.6 Load transfer efficiency measurement (a) falling weight deflectometer device (b) falling weight deflectometer weight and deflection sensors.

The FWD device recorded two LTE values that correspond to each joint: the approach LTE and the leave LTE. A schematic illustrating the process for recording the approach and leave LTE values at a typical joint is shown in Figure 2.7. The figure shows where the weight was applied for each corresponding reading and the locations of the deflections used for calculations.

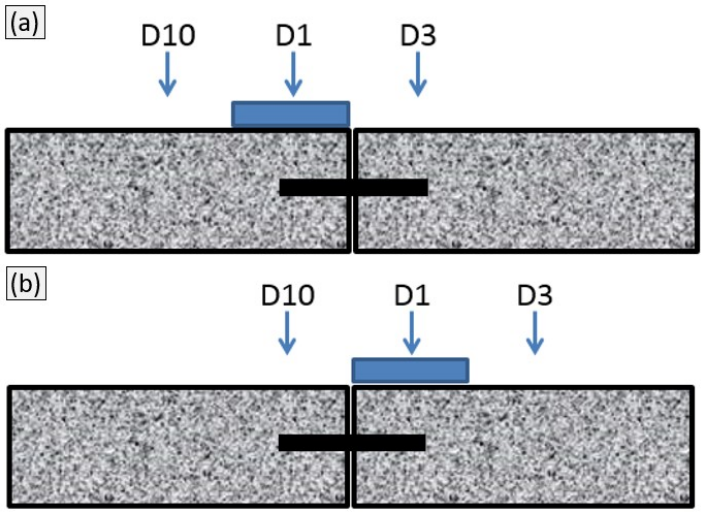

Figure 2.7 Standard falling weight deflectometer process for recording/calculating: (a) approach and (b) leave load transfer efficiency values.

The equations 1 and 2 show the calculation for pavement approach and pavement leave LTEs, respectively.

$$Load\ transfer\ efficiency = \frac{D3}{D1} * 100\% \quad (1)$$

$$Load\ transfer\ efficiency = \frac{D10}{D1} * 100\% \quad (2)$$

where D1, D3, and D10 are deflections at associated part of the pavement.

The existing sub-cells which were repaired within the scope of this report consisted of three joints, each of these joints were removed and replaced with a patch containing the dowel bar repairs being analyzed within this report, creating an additional three joints for each sub cell. The new configuration for the FWD process accounting for these additional joints is shown in Figure 2.8.

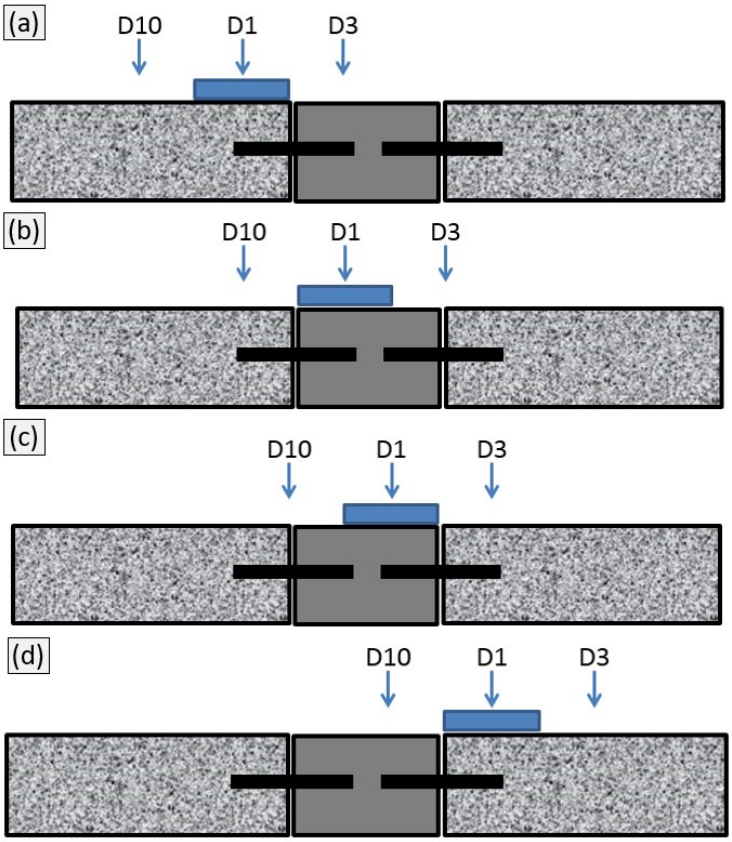

Figure 2.8 Falling weight deflectometer process for recording/calculating approach and leave load transfer efficiency values for sub cells: (a) pavement approach, (b) patch leave, (c) patch approach, (d) pavement leave.

The equation 1 was used for pavement and patch approach LTE values while equation 2 was used for pavement and patch leave LTE values.

2.2 Evaluation Process

The traffic volume of the Old Westbound was recorded with Weigh in Motion devices. Within the scope of this report, it was consequently possible to correlate traffic volume or age to the performance of the individual epoxy/grout dowel system in comparison to the others to ascertain initial performance and long-term performance of the various epoxy/grout systems. However, after only 5 years, it was premature to relate performance to traffic, but the FWD results, and ride trends were evaluated to ascertain trends that were indicative or reflective of the performance of each factorial of the experiment. Traffic comparison between lanes (driving versus passing lanes) was confounded by post-construction grinding of the driving lane only.

Researchers considered ride measurement, FWD results, and forensic coring to be germane. FWD and ride measurements were conducted seasonally on the test cells. Ride quality was measured using the lightweight profiler, which was later equipped with two GOCATOR accelerometers (replacing the TriODS and ROLINE lasers), by operating the device through the 13 contiguous cells from the east end of Cell

970 to the west end of Sub Cell 982. Utilizing the FHWA ProVAL software, the international roughness index for each cell was analyzed by cropping each cell as a segment of the continuous measurement.

Chapter 3: Results

3.1 Scheme

Within the thirteen sub cells, six different dowel repair processes were evaluated, along with one control cell with no repairs (Figure 2.3). There were two sub cells for every repair method, one using 1 inch diameter dowel bars and the other using 1.25-inch diameter dowel bars. Table 3.1 details the dowel attachment methods used for each cell.

Table 3.1 Reference chart for dowel attachment methods for each sub cell

Cell	Material
970[a]	No grout
971[b]	No grout
972 [a]	Bag injected grout
973 [b]	Bag injected grout
974 [a]	Dip grout
975 [b]	Dip grout
976 [a]	Capsule grout
977 [b]	Capsule grout
978 [a]	Epoxy Experimental 2
979 [b]	Epoxy Experimental 2
980 [a]	Epoxy Experimental 1
981 [b]	Epoxy Experimental 1
982 [a]	Control

[a] 1-inch dowel bar, [b] 1.25-inch dowel bar.

3.2 Ride Quality (IRI) Results

IRI is an indicator of pavement condition, particularly those affected by certain wavelengths and waveforms. In a 27-foot joint interval, the dominating waveform is easily this joint interval, but additional factors due to joint condition are extant. The initial ride quality profiles of the test cells were collected during the spring and fall of 2015. Subsequent measurements were collected in 2017 and 2018. Ride quality data was recorded on both driving and passing lanes, making it possible to compare the IRI values between lanes. It is worth noting that the driving lane was diamond ground following repairs, while the passing lane was left alone, providing an initially lower IRI value for the driving lane. Over the course of IRI measurements, the driving lane IRI increased greatly compared to the passing lane, suggesting that traffic had an effect on IRI.

Based on measurements, it appeared initially that the no grout sub cells performed almost similarly with the various grouting alternatives. It is believed that the mechanism of load transfer may be more complex in the sense that dowels that were not over-encastered but free in direction and not in rotation were probably more capable of transmitting deflection. The grout capsule method, which did best in the

previous in-house experiment, appeared validated in the test sub cells as average mostly for the smaller diameter dowel bars (1 inch dowel bar). Figure 3.1 and Figure 3.4 provide a comparison between the initial spring and fall IRI for the test cells. In general, within each pair of grout or epoxy fixes, the larger diameter dowel bars generally exhibited higher IRI than the smaller diameter dowel bars in the driving lane. In the driving lane, IRI mostly stayed the same or decreased after 7 months with both TriODS and ROLINE lasers as shown in Figure 3.1 and Figure 3.3, respectively. In the passing lane, IRI mostly decreased after 7 months similar to the driving lane Figure 3.1 and Figure 3.3.

In the repairs utilizing Epoxy Experimental 1 (Sub Cells 980 and 981), the larger diameter bars (sub cell 981) exhibited better ride quality than the smaller diameter bar (sub cell 980) for the driving lane (Figure 3.1 and Figure 3.3) while it was observed to be opposite for the passing lanes (Figure 3.2 and Figure 3.4). The investigation of the mechanism causing the observed outcome is not within the scope of this study. However, the authors suggest that a larger diameter may result in excessive bearing area, which could potentially interfere with the variation in diameter. This interference could be either a confounding factor, or it could indicate that the larger diameter indeed has excessive bearing area.

Since there were only two field test dates initially, it was difficult to make definitive conclusions to how the IRI values change over time. A longer-term evaluation provided the results in Figure 3.5 to Figure 3.8, where in the driving lane the lowest IRI, and therefore most ideal values, overall came from Cell 981 followed by Sub Cell 980, both of which were the repairs utilizing Epoxy Experimental 1. Meanwhile the highest, and worst IRI values came from Sub Cells 971 and 970, the no grout cells. The control Sub Cell 982, tended toward the median of the IRI scatter of the driving lane. The passing lane IRI values were overall closer together than in the driving lane, and the IRI values were in general more random, suggesting that the lack of traffic in this lane prevented the differences in repair methods and materials from having a significant effect on ride quality.

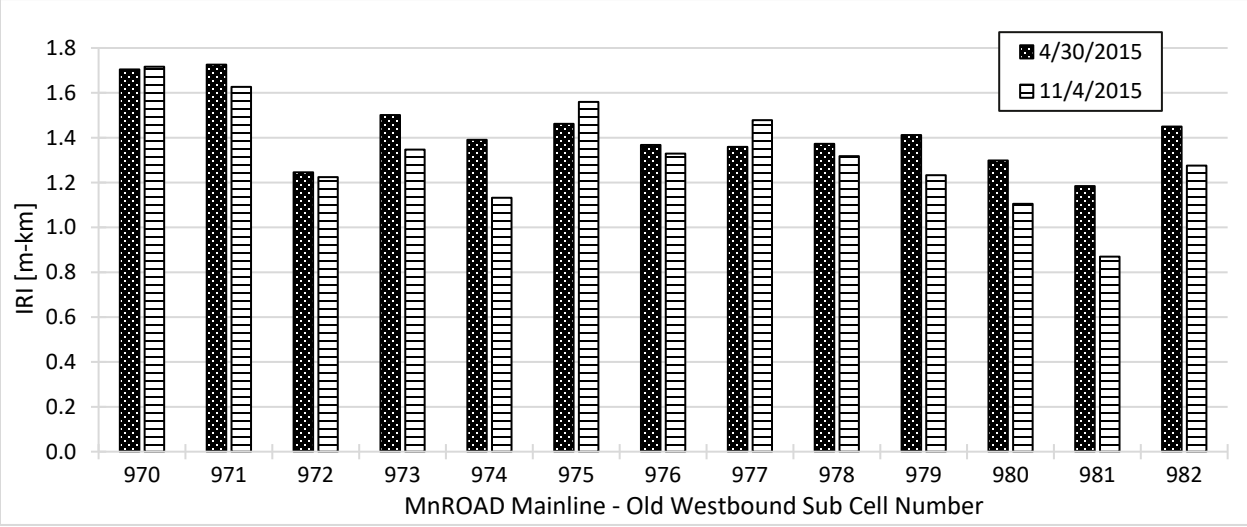

Figure 3.1 Spring and fall driving lane TriODS International Roughness Index (IRI) values for the various test cells.

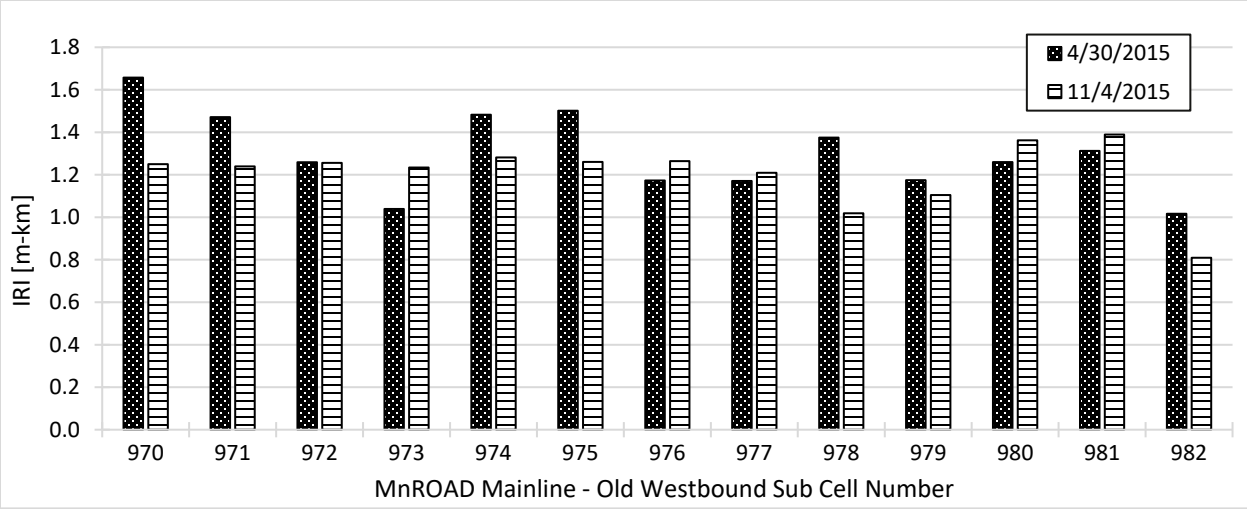

Figure 3.2 Spring and fall passing lane TriODS International Roughness Index (IRI) values for the various test cells.

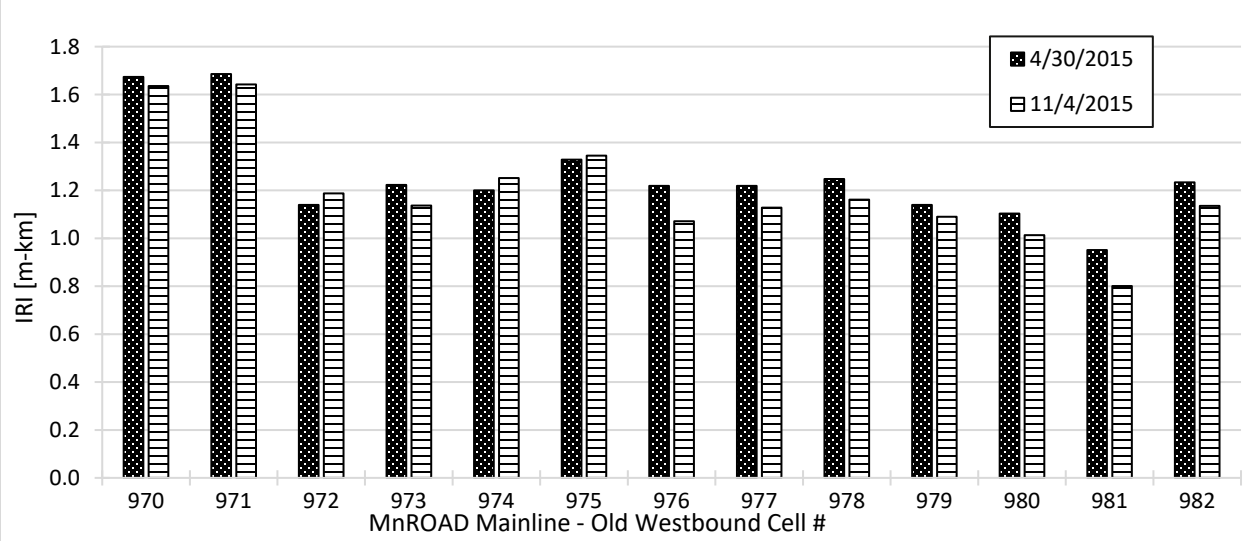

Figure 3.3 Spring and fall driving lane ROLINE International Roughness Index (IRI) values for the various test cells.

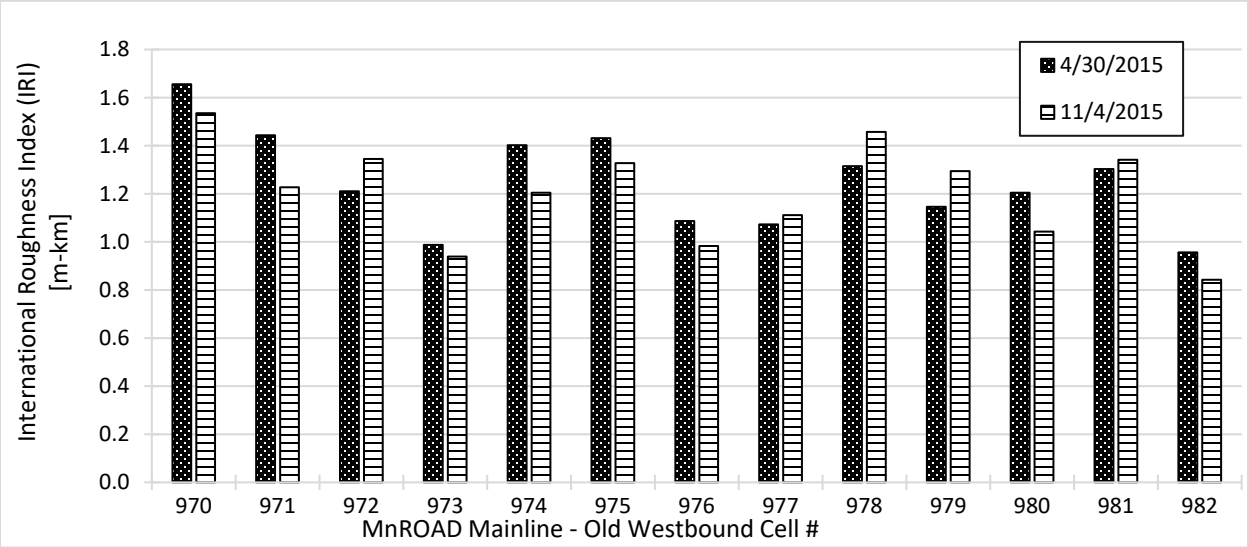

Figure 3.4 Spring and fall passing lane ROLINE International Roughness Index (IRI) values for the various test cells

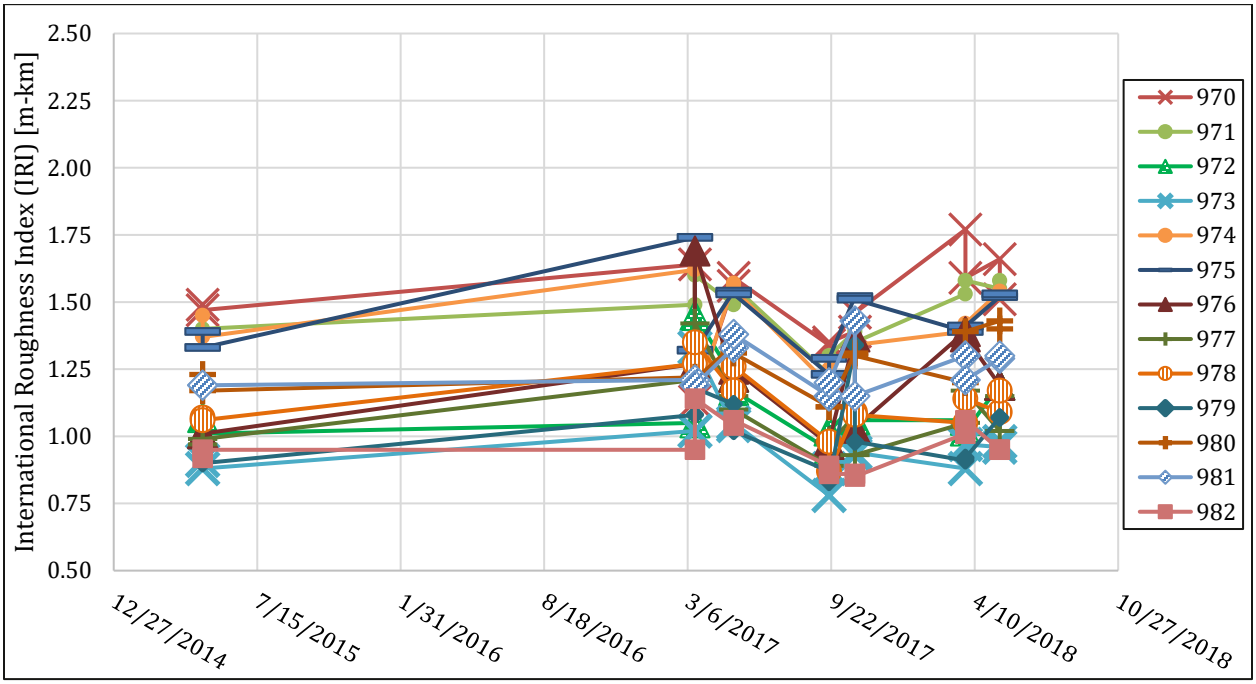

Figure 3.5 Passing lane left wheel path (LWP) International Roughness Index (IRI).

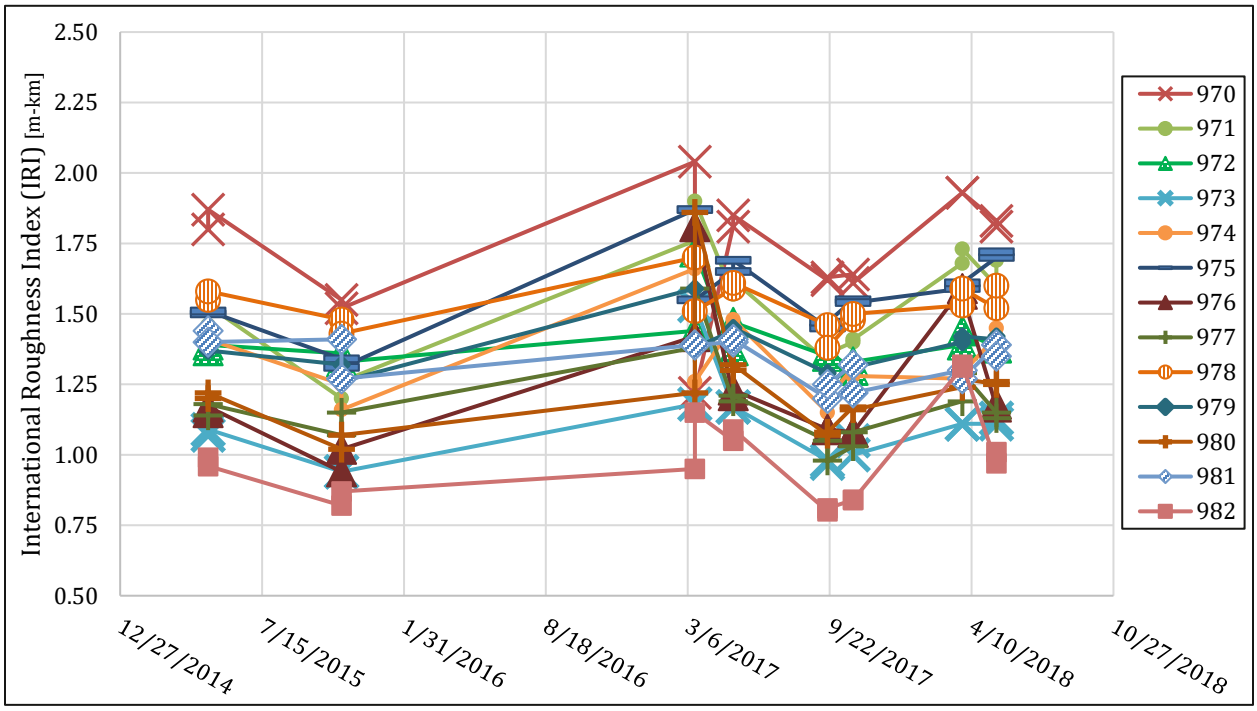

Figure 3.6 Passing lane right wheel path (RWP) International Roughness Index (IRI).

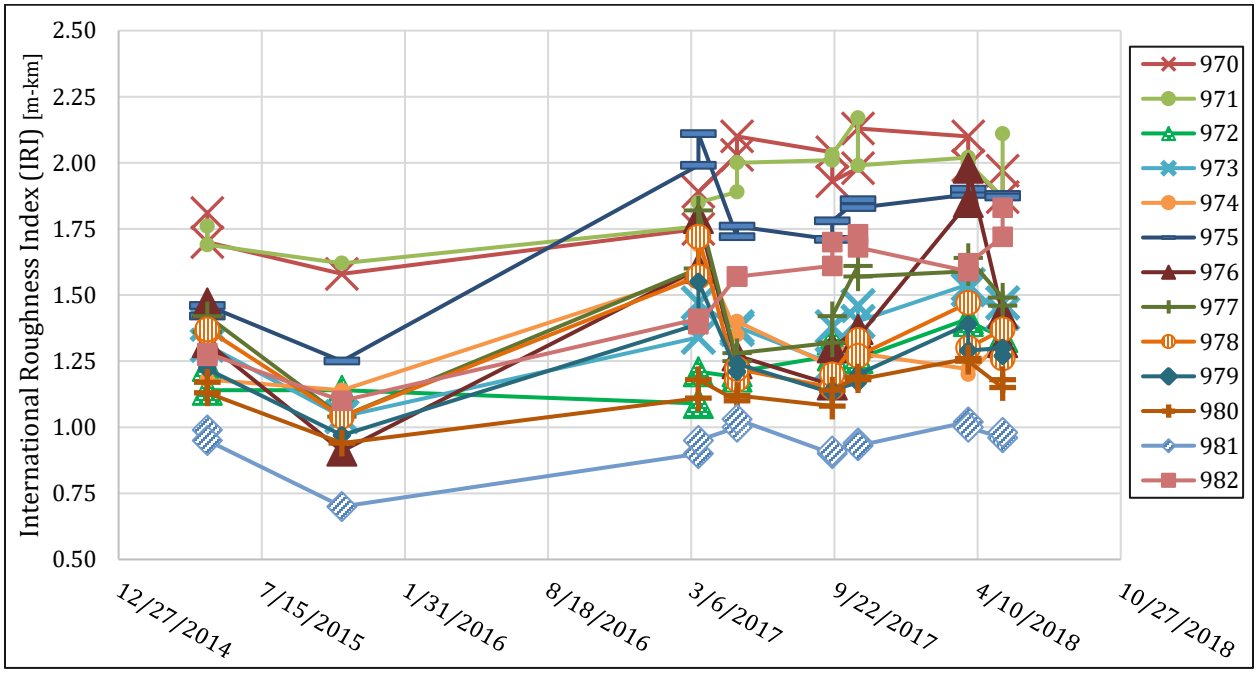

Figure 3.7 Driving lane left wheel path (LWP) International Roughness Index (IRI).

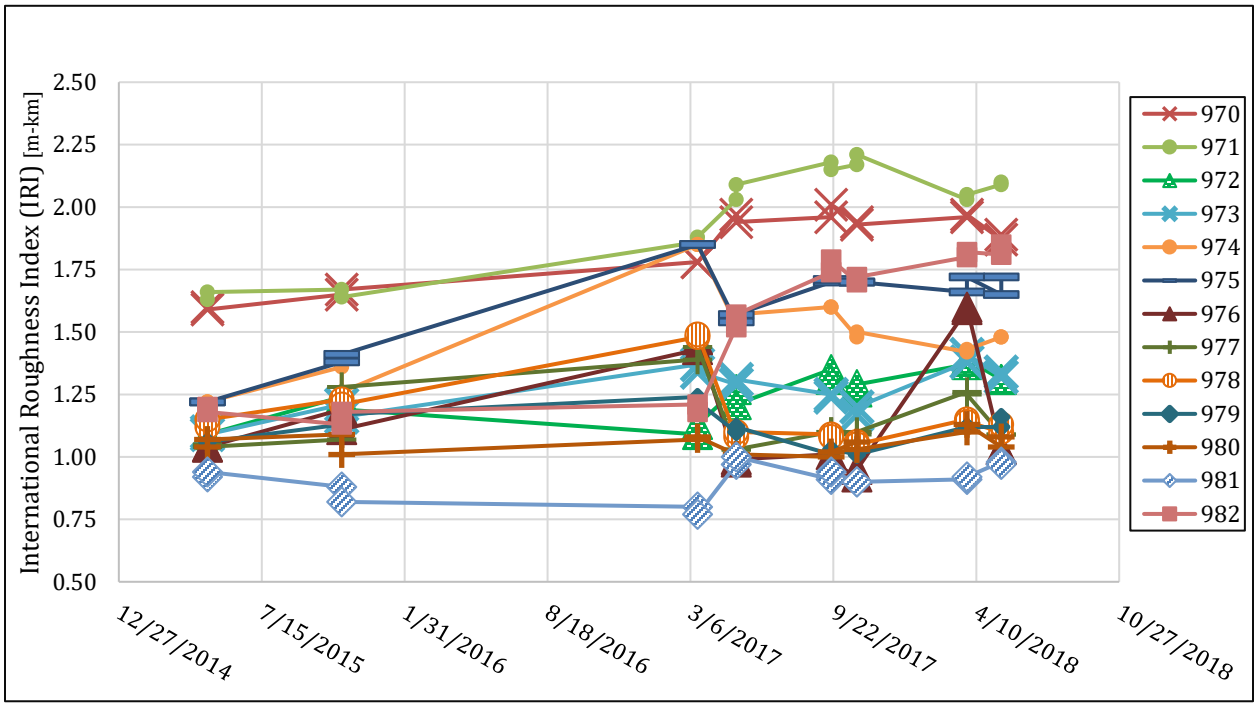

Figure 3.8 Driving lane right wheel path (RWP) International Roughness Index (IRI).

3.3 Joint Load Transfer Test Results

The volume of data collected for the joint LTE of the test sub cells significantly exceeded that of IRI data. The plethora of field test dates allowed for a clearer performance trend to be generated for the LTE. In this experiment, the FWD device only gathered LTE values corresponding to the driving lane on the test sub cells. The deflection measurements for loading from all nine field test dates, including the data collected prior to the installation are given in Figure 3.9 to Figure 3.12. The installation date of the dowel repair experiment (8/16/2013) was integrated into these graphs.

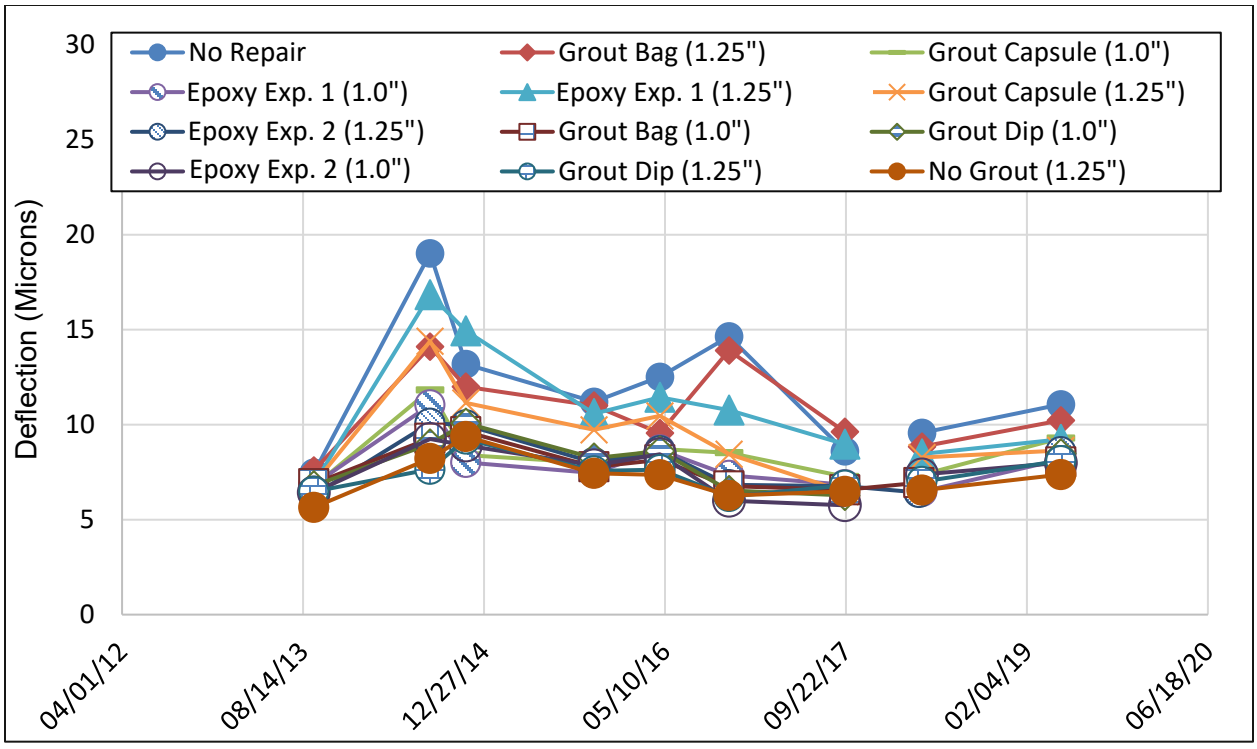

Figure 3.9 Deflection measurements for loading on patch approach side

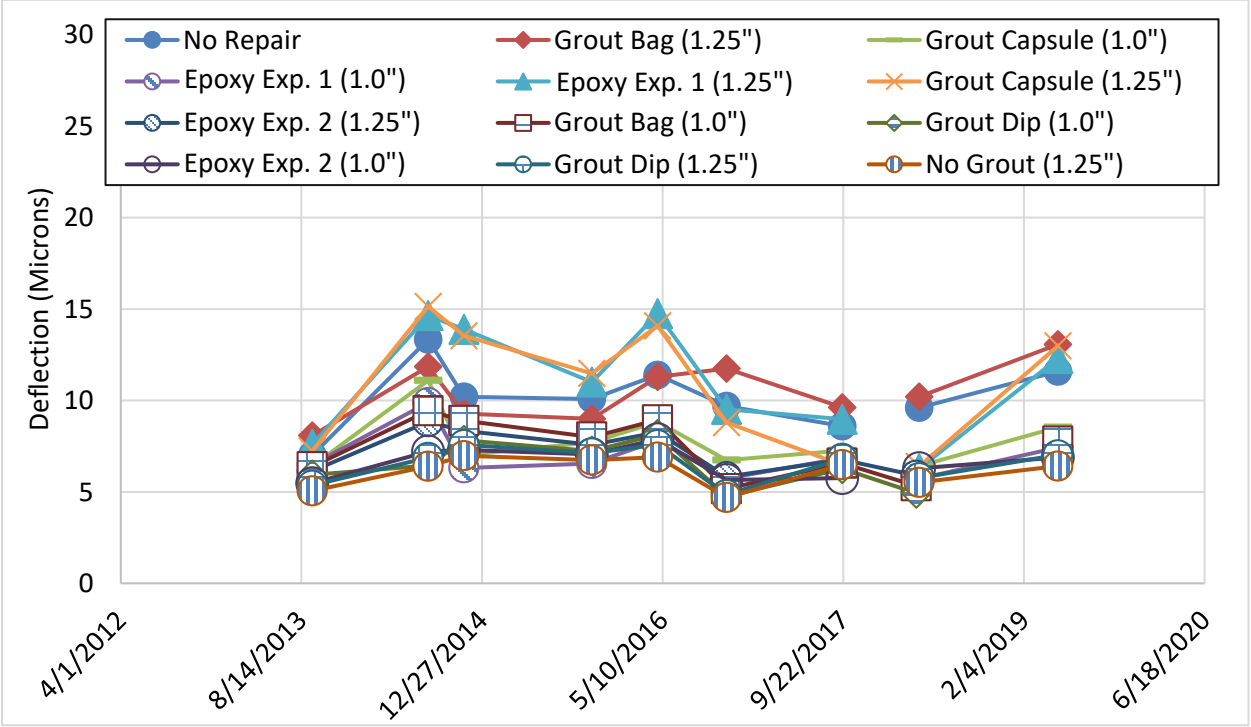

Figure 3.10 Deflection measurements for loading on patch leave side

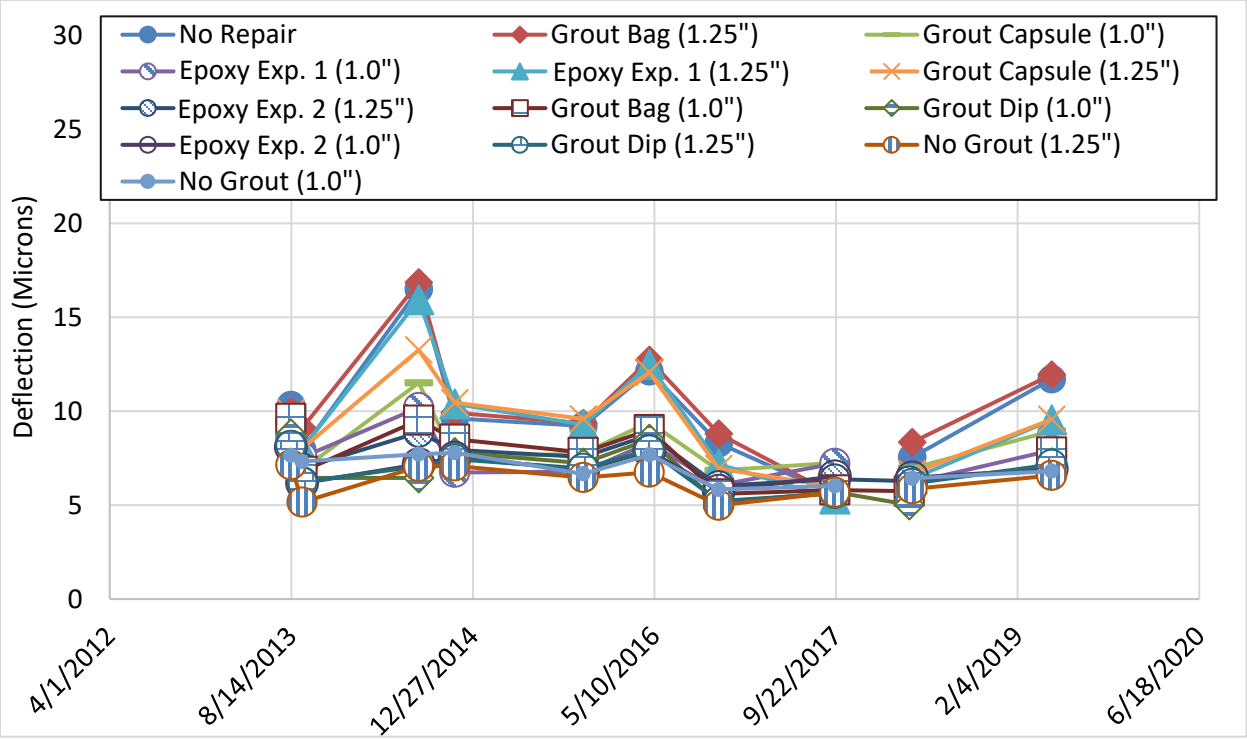

Figure 3.11 Deflection measurements for loading on pavement approach side

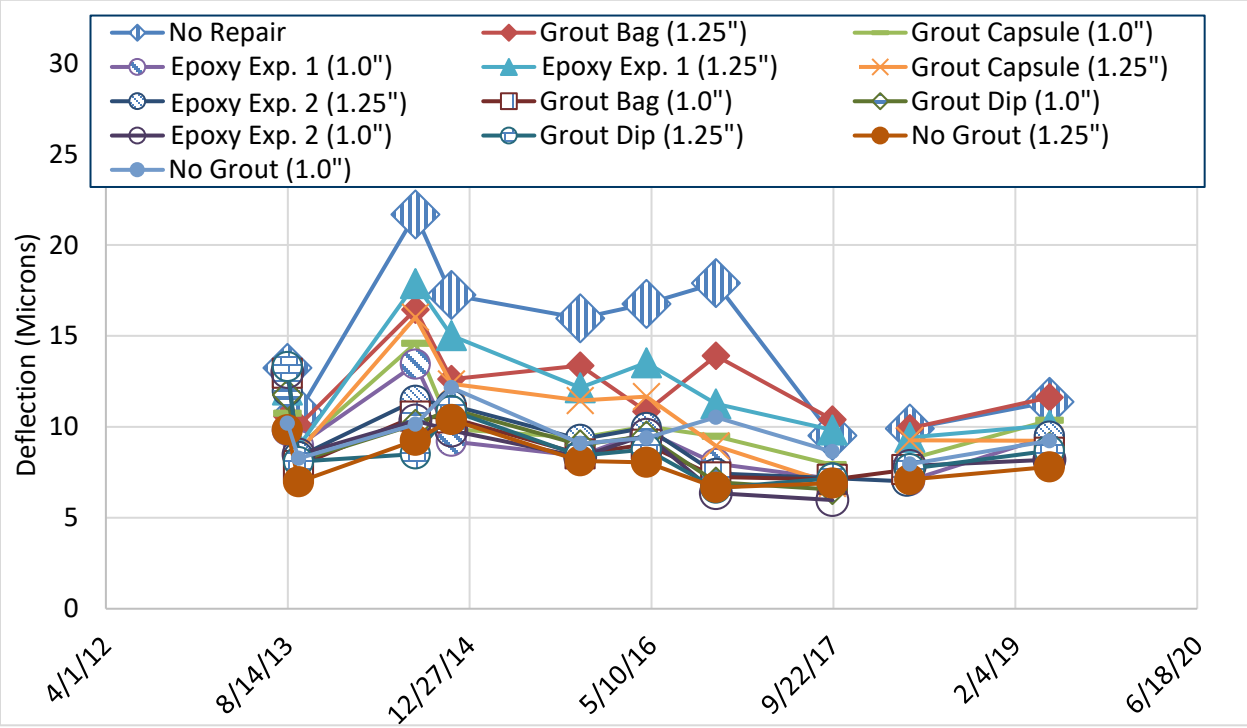

Figure 3.12 Deflection measurements for loading on pavement leave side

For simplification, Figure 3.13 and Figure 3.19 show separate graphs for the type of dowel repair method used for each Sub Cell. These were also split into leave and approach LTE values (refer to Figure 2.8). These figures directly compare the LTE values for each dowel repair method, as well as the different diameters (1" and 1.25") of the same repair type.

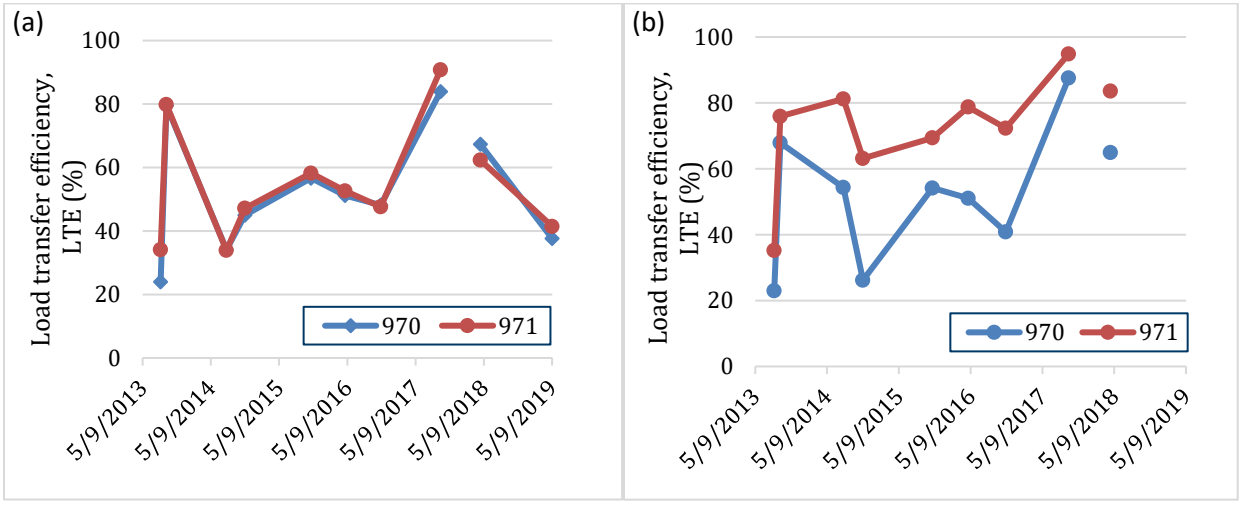

Figure 3.13 General time trend for load transfer efficiency (LTE) of sub cells without grout: (a) approach, (b) leave).

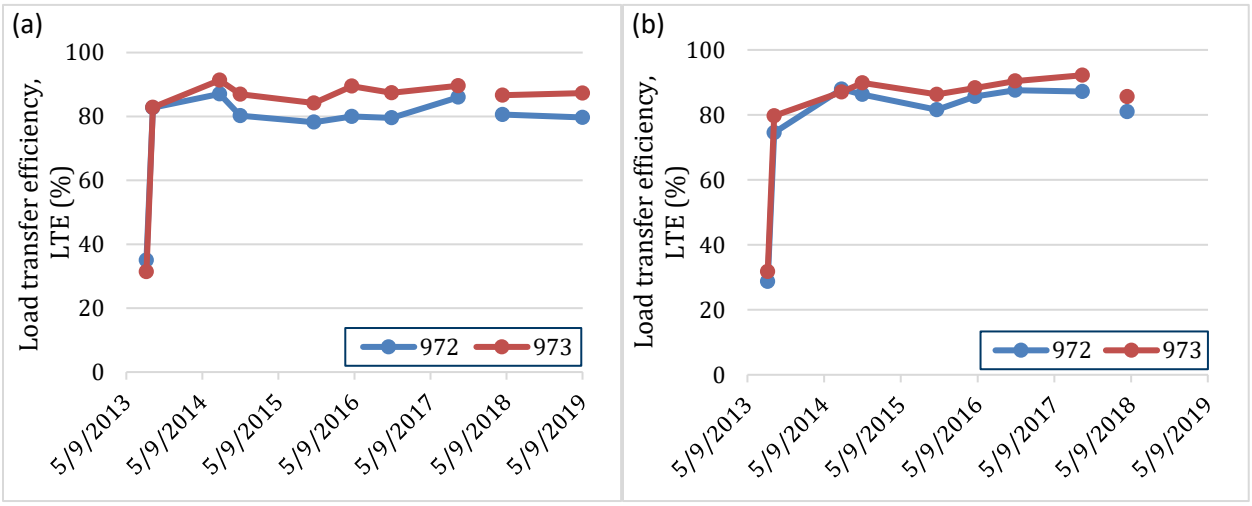

Figure 3.14 General time trend for load transfer efficiency (LTE) of sub cells using the grout - bag injection method: (a) approach, (b) leave.

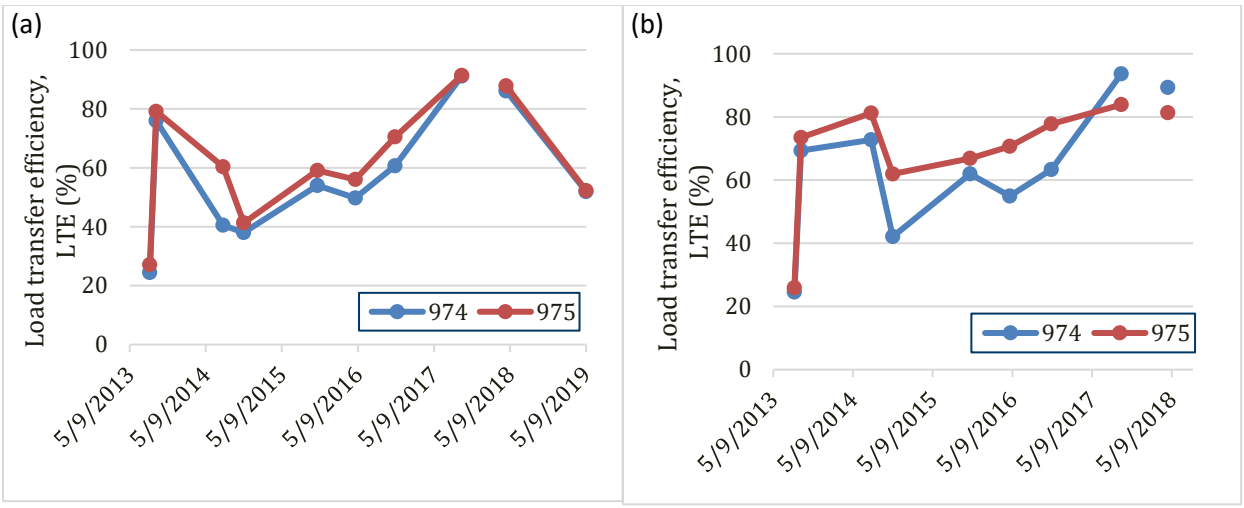

Figure 3.15 General time trend for load transfer efficiency (LTE) of sub cells using the grout - dip method: (a) approach, (b) leave.

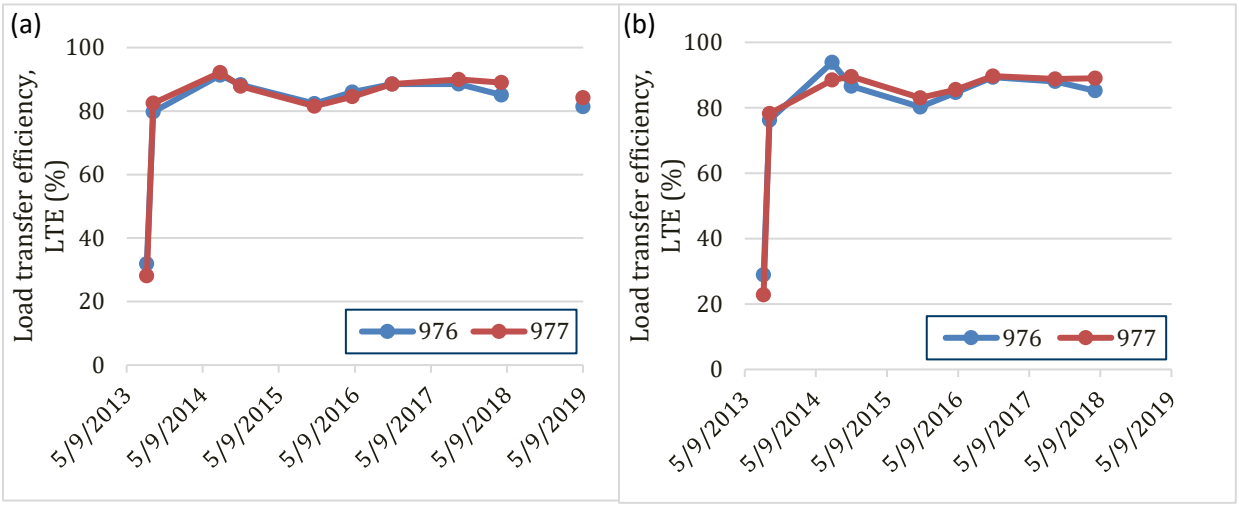

Figure 3.16 General time trend for load transfer efficiency (LTE) of sub cells using the grout - capsule method: (a) approach, (b) leave.

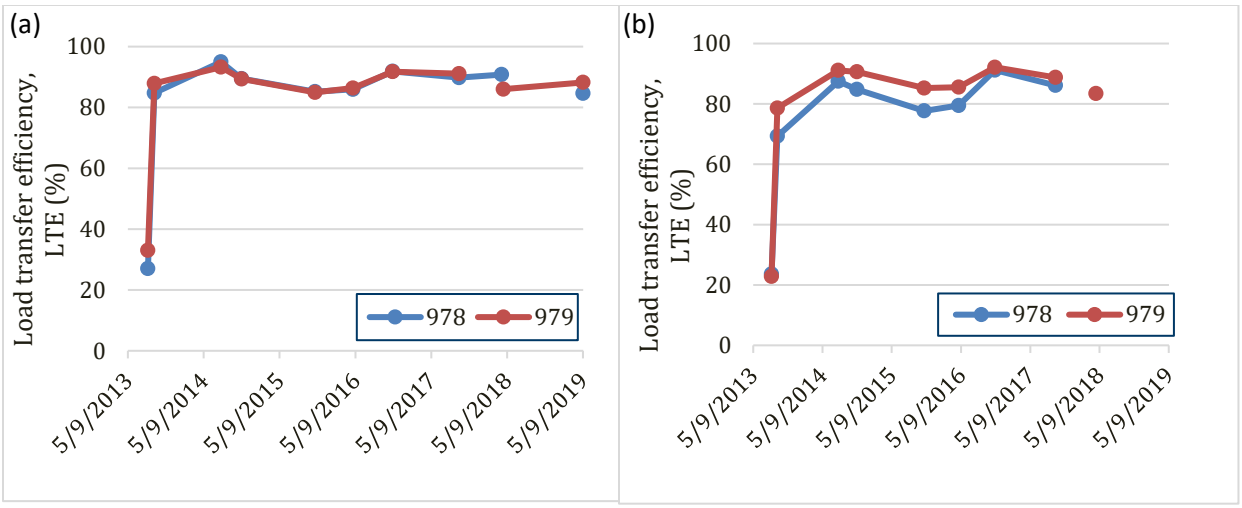

Figure 3.17 General time trend for load transfer efficiency (LTE) of sub cells using epoxy experimental 2: (a) approach, (b) leave.

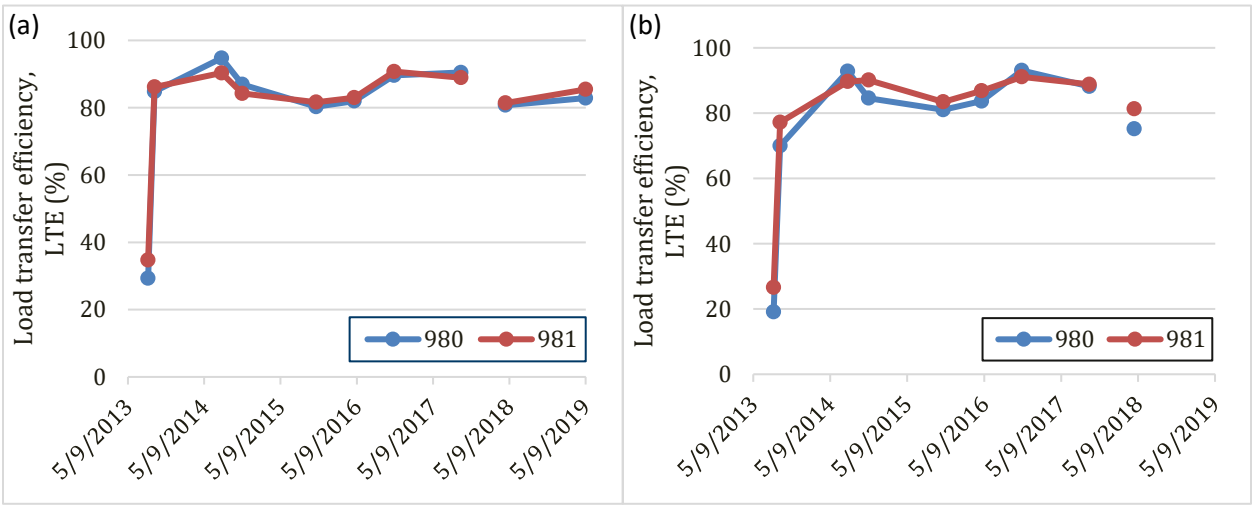

Figure 3.18 General time trend for load transfer efficiency (LTE) of sub cells using epoxy experimental 1: (a) approach, (b) leave.

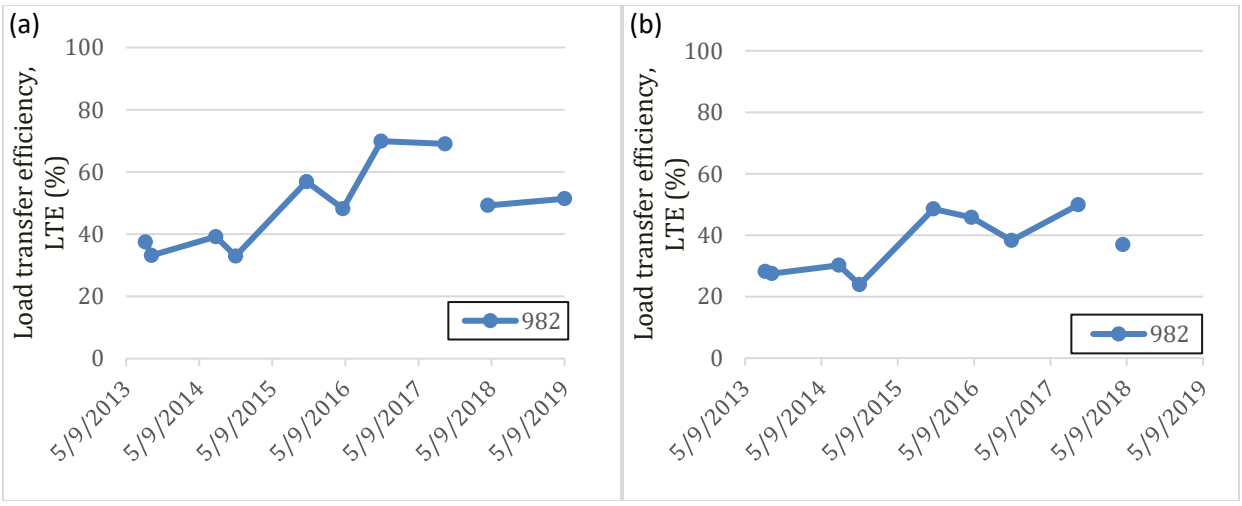

Figure 3.19 General time trend for load transfer efficiency (LTE) of sub cell experiencing no repair: (a) approach, (b) leave.

A more intelligible analysis of the general time trends for LTE were obtained when disregarding the LTE values from the 8/13/2013 field test. This provided a better understanding of how the LTE values changed from each field test date after the installation, and which sub cells produced the best and the worst LTE values. The following graphs (Figure 3.20 to 3.22) disregard the LTE data collected on 8/13/2013 and were separated corresponding to their respective adhesive method. All of the figures that were constructed in regard to the LTE data were separated with respect to their adhesive method used for the dowel repair. This separation only allowed for a direct comparison between a few sub cells at a time. Two collective models displaying the approach and leave LTE results from every field test for every test cell were generated. These models directly compared all sub cells involved in this experiment. As shown in Figures 3.20 to 3.22 the sub cells using the grout – dip method produced LTE values much smaller than the other two dowel repair methods utilizing grout. To account for this difference, the grout – dip method test cells have been modeled with the other test cells using dowel repair methods that produced inadequate LTE values (i.e., test sub cells using dowels with no grout and test cells with no repair) in Figure 3.22.

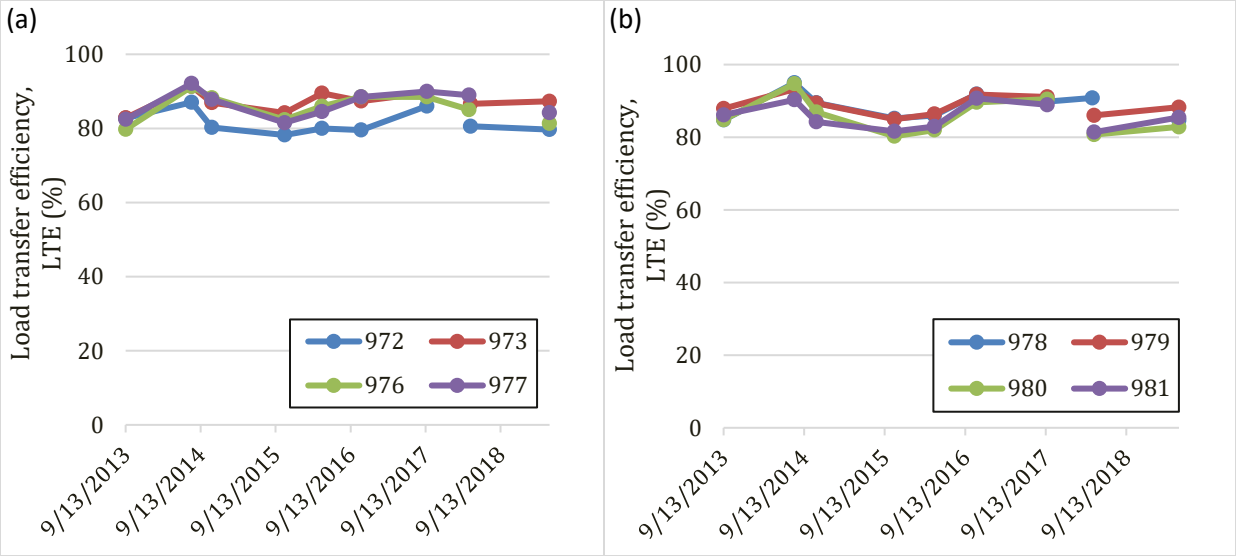

Figure 3.20 General time trend for load transfer efficiency (LTE) approach values: (a) grout, (b) epoxy methods.

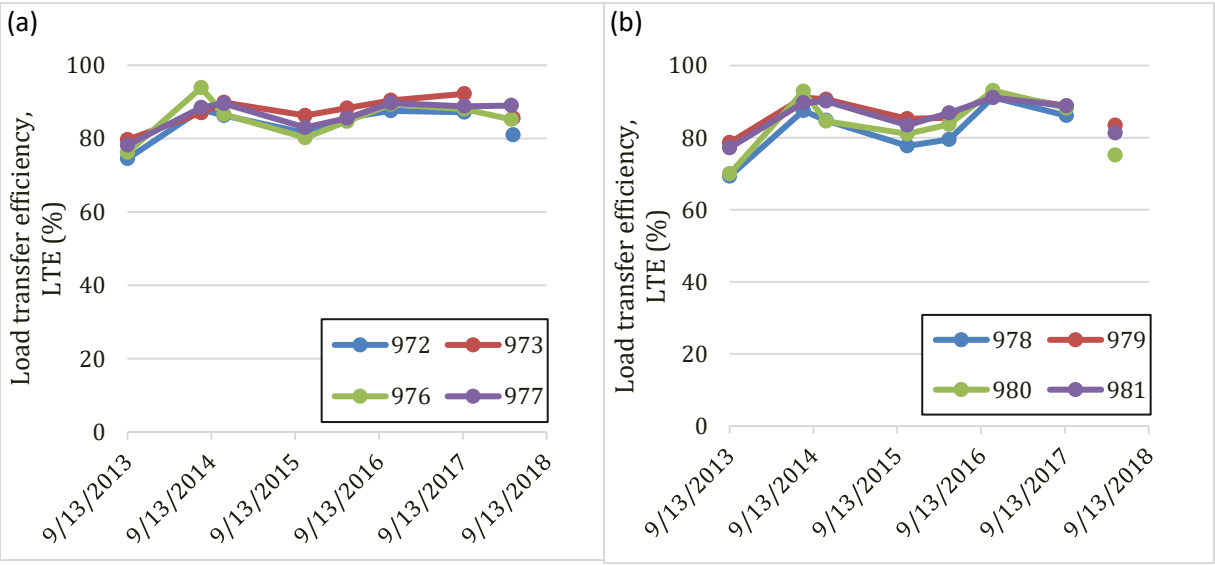

Figure 3.21 General time trend for load transfer efficiency (LTE) leave values (a) grout, (b) epoxy methods.

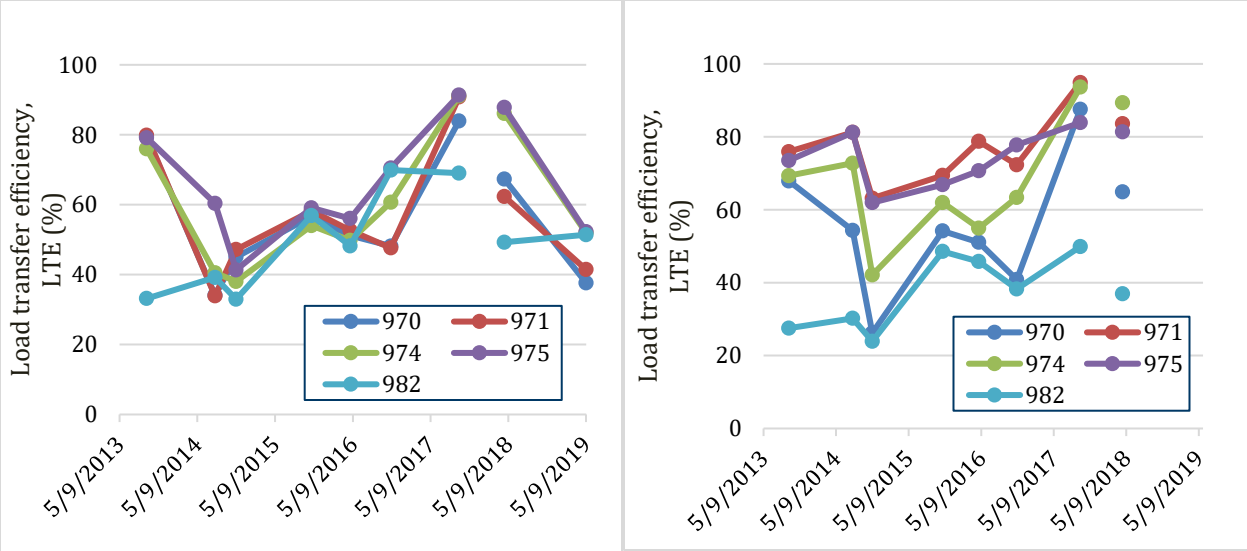

Figure 3.22 General time trend for low load transfer efficiency (LTE) value sub cells (a) approach, (b) leave.

3.4 Applied Traffic

Traffic loads typically influence pavement performance. When performing an experiment similar to the experiment discussed in this report, it is essential to obtain and understand the traffic data that the analyzed pavement area experiences. Table 3.2 displays the traffic data for the driving and passing lane on the Old I-94 Westbound section from the previous four years following to dowel bar repair. This dataset enabled an understanding of why data from a specific field test, conducted during a particular year, exhibited signs of being an outlier compared to data from other field tests conducted in different years. However, it should be noted that this table lacks specification regarding the timing of the traffic days throughout the year. This absence of information makes it difficult to establish definitive correlations between the traffic impact and the observed variations in LTE and IRI.

Table 3.2 MnROAD Old I-94 Westbound traffic data.

Year		2013	2014	2015	2016
Total Days		365	365	365	366
Traffic Days		37	66	58	166
Driving Lane	AADT (1-way)	1376	2393	2237	6165
	HCADT	317	539	494	1361
	% Trucks	23.0	22.5	22.1	22.1
	BESALs	103992	182561	165342	468941
	CESALs	157118	276124	250049	711805
Passing Lane	AADT (1-way)	1336	2479	2348	6409
	HCADT	88	156	149	419
	% Trucks	6.6	6.3	6.4	6.5
	BESALs	27748	48485	44810	108788
	CESALs	41569	72532	66774	157658

3.5 Visual Results

Thirteen cores were taken from Cells 970 through 982 for visual observation. Images of these cores are provided in Figure 3.23 and Figure 3.24. The core for Cell 970 was taken with the dowel on the side of the core which explains why only one side provides view of the dowel. Observations from the cores included the amount of concrete breakdown around the dowel, evenness of the grout or epoxy suspending the dowel within the hole, and the degree of void space surrounding the dowel. Quality was recorded under three categories of Good, Marginal, and Bad as shown in Table 3.4 along with the visual observation notes. These condition results were organized into counts for Table 3.4 to 3.6 to better compare the quality produced by differing dowel sizes, bonding materials, and overall methods.

Figure 3.23 Front view of cores from sub cells 970 through 982 (left to right).

Figure 3.24 Back view of cores from sub cells 970 through 982 (left to right)

As can be seen from Figure 3.23 and Figure 3.24 the core from sub cell 982 contains a large transverse crack across it. In recent years, cores extracted from older dowelled concrete structures have exhibited comparable patterns of cracking to those observed in the provided example. This may be caused by the need for stress release in the dowel, which normally manifests as a breakdown of the concrete surrounding the dowel but, in some cases, manifests as major transverse cracking.

Table 3.3 Visual results for cores taken in Sub Cells 970 through 982

Cell	Material	Condition	Notes
970	No grout	Good	No deterioration at the interface
971	No grout	Marginal	Some deterioration of the concrete around the dowel.
972	Bag injected grout	Good	No concrete breakdown and overall even appearance of dowel in grout.
973	Bag injected grout	Marginal	Dowel not centered, no breakdown of concrete.
974	Dip grout	Bad	Spacing uneven around dowel with some breakdown of the concrete.
975	Dip grout	Bad	Lots of space without grout and mild concrete breakdown.
976	Capsule grout	Marginal	Very mild void spaces with uneven dowel.
977	Capsule grout	Good	Mild unevenness and small voids.
978	Epoxy Experimental 2	Good	Mild unevenness and small voids.
979	Epoxy Experimental 2	Marginal	Mild voids, but severely uneven, dowel completely flush with wall.
980	Epoxy Experimental 1	Good	No voids and dowel is very evenly placed.
981	Epoxy Experimental 1	Good	Mild voiding and mild unevenness of the dowel.
982	Control	Bad	Major transverse cracking with small voids, dowel rusted (At least 40 years old).

Based on the data presented in Table 3.4, it can be observed that the 1-inch dowels mostly demonstrate a more favorable visual outcome compared to the 1.25-inch dowels. The overall counts trend towards the "Good" category, indicating better performance with the 1-inch dowels.

Table 3.4 Cell quality counts comparing dowel size, not including Sub Cell 982.

	Good	Marginal	Bad
1”	4	1	1
1.25”	2	3	1

Table 3.5 shows the number of Good, Marginal, and Bad sub cells by their bonding materials. The grout bonding material had 2 sub cells in each quality category and the “None” category had 1 in each. However, the epoxy appeared to have a better rating, as it had 3 sub cells in the “Good” category with 1 in the Marginal.

Table 3.5 Cell quality counts comparing bonding material.

	Good	Marginal	Bad
Epoxy	3	1	0
Grout	2	2	2
None	1	1	1

Table 3.6 compares the quality of sub cells based on their overall treatment type. Most of the treatments had one sub cell each in the Good and Marginal categories, while the Dip Method and Control both had all their sub cell in the Bad category and the Epoxy Experimental 1 had both cells in the Good category.

Table 3.6 Cell quality counts comparing all treatment types.

	Good	Marginal	Bad
No Grout	1	1	0
Bag Injected	1	1	0
Dip Method	0	0	2
Capsule Method	1	1	0
Epoxy Experimental 2	1	1	0
Epoxy Experimental 1	2	0	0
Control	0	0	1

3.6 Faulting Measurement Using the MnROAD Digital Faultmeter

Faulting in pavements is defined as the relative at rest difference in elevation between 2 sides of a joint presenting especially as a distress form. Typically, the leave side of the joint is higher than the approach

side. Faulting is usually the result of a poorly designed joints, rocking panels , insufficient load transfer mechanism, a bad base, poor aggregate interlock at the joints and the progressive action of loss of erodible and transportable base materials from the approach panel to the leave panel. Consequently, in a rear-view survey one can easily see faulting ordinarily. In very rare instances can faulting be visible in a wind shield survey. MnDOT uses a Digital Faultmeter designed and built at MnROAD for MnROAD. The MnROAD Digital Faultmeter Version 2.0 (MDF2) was constructed at MnROAD in 2021 (Figure 3.25). The MnDOT Faultmeter is a simple device howbeit an improvement over the Georgia Faultmeter. It is equipped with an alignment laser and a measurement laser that stay on while the equipment is measuring faulting.

Faulting is usually mitigated by diamond grinding but if the cause is base related or the result of rocking panels, diamond grinding provides only a transient / ephemeral solution.

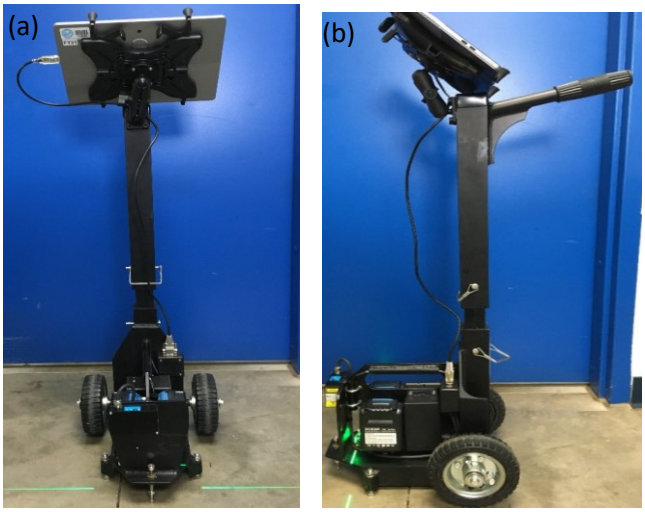

Figure 3.25 MnROAD Digital Faultmeter: (a) front (b) side.

It was important to evaluate the test cells using faulting as a criterion. As can be seen in Figure 3.29 and 3.27 , various joint measurements were conducted in the test cells taking care to note pavement approach or pavement leave so that the relevant anchored dowels were evaluated.

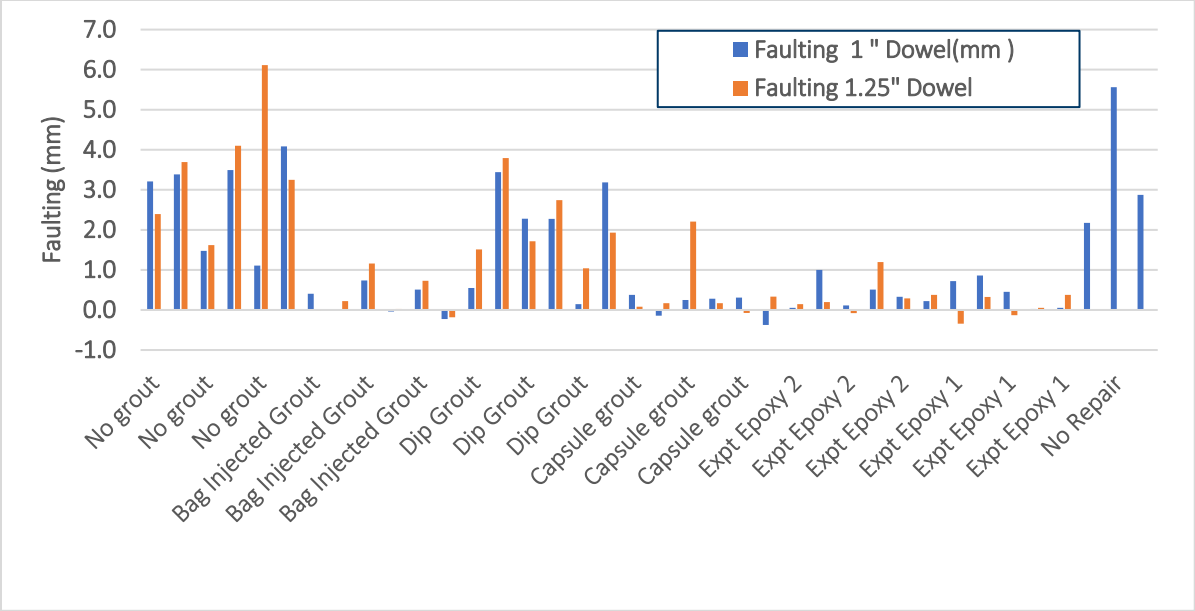

Figure 3.26 Comparison of faulting in cells with 1" diameter dowels to corresponding cells with 1.25" diameter dowels.

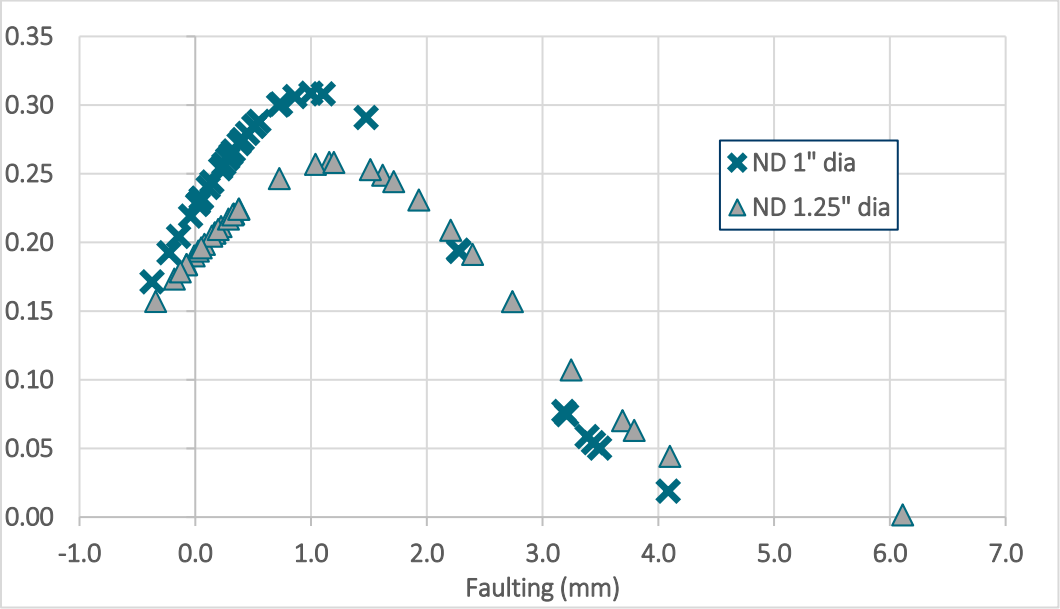

Figure 3.27 Normal Distribution of Faulting in 2 different Dowel sizes

The statistical analysis are shown in Tables 3.7 and 3.8.

Table 3.7 Descriptive statistics result of the measured faulting

	Faulting 1 " Dowel (mm)	*Faulting 1.25" Dowel (mm)*
Mean	1.002	1.175
Standard Error	0.217	0.258
Median	0.452	0.376
Mode	#N/A	#N/A
Standard Deviation	1.284	1.528
Sample Variance	1.648	2.335
Kurtosis	0.122	1.947
Skewness	1.228	1.482
Range	4.458	6.454
Minimum	-0.373	-0.342
Maximum	4.086	6.112
Sum	35.074	41.140
Count	35.000	35.000
Largest(1)	4.086	6.112
Smallest(1)	-0.373	-0.342
Confidence Level (95.0%)	0.441	0.525

Table 3.8 t-Test: Paired Two Sample for Means

	Faulting 1 " Dowel (mm)	*Faulting 1.25" Dowel (mm)*
Mean	1.002113502	1.175421
Variance	1.647900905	2.335043
Observations	35	35
Pearson Correlation	0.730469165	
Hypothesized Mean Difference	0	
df	34	
t Stat	-0.97005347	
P(T<=t) one-tail	0.16943524	
t Critical one-tail	1.690924255	
P(T<=t) two-tail	0.338870479	
t Critical two-tail	2.032244509	

3.7 Discussion

3.7.1 Analyses of Ride Information

Ride quality data was measured on both driving and passing lanes on the Old Westbound 94 section, to compare the IRI values between lanes anticipating that the passing lane for each test section should produce a lower IRI value than the driving lane, due to it receiving a lower volume of heavy vehicles. The comparison was further confounded by the fact that only the driving lane received diamond grinding. The TriODS and ROLINE IRI values for both lanes fall between 0.8 and 1.75 [m-km]. The obtained IRI values were decent, but not ideal for a pavement. These ride quality tests were conducted approximately one and a half years and two years after the initial implementation of this experiment, which may subsequently be the reason for these non-ideal IRI values. Additionally, the process for dowel repairs did not address any of the issues or distresses that may have been present in between the joints. These potential distresses would have contributed significantly to the IRI recorded for the test cells. From Figure 3.1 andFigure 3.4, the general time trend for IRI appeared to show the majority of sub cells decreasing in IRI from spring to fall in 2015. Figure 3.1 and Figure 3.3 show over 75% of sub cell IRI values decreased from the spring to the fall, and Figure 3.2 and Figure 3.4 show over 50% of sub cell IRI values decreased from the spring to the fall. This data did not align with the expected general time trends for IRI values. With the addition of data from other field test dates, there may be more evidence of a trend that more closely resembles the trend that was expected.

When comparing the IRI data from the driving lane to the passing lane, it is important to keep in mind that the procedure of this experiment involved diamond grinding only on the driving lane of the repaired sub cells. This can potentially explain why the driving lane IRI values were lower than the passing lane IRI values for some of the sub cells, regardless of the driving lane experiencing a larger volume of heavy vehicles. Diamond grinding is a prominent practice when implementing concrete pavement repairs, making the driving lane data a more accurate representation of the ride quality performance of the repaired sub cells. The sub cells that provided the best ride quality for the driving lane and passing lane are Sub Cells 981 and 982, respectively. The sub cells that produced the worst ride quality for the driving lane and passing lane were Sub Cells 971 and 970, respectively.

Sub Cells 970 and 971 were consistently producing amongst the worst ride quality data. This suggested that inserting dowels with no anchoring had the most negative effects on the ride quality experienced by drivers in comparison to the other repair methods analyzed. The figures also made it evident that Sub Cells 980 and 981 provided the optimal driving lane IRI values, and Sub Cell 982 provided the optimal passing lane IRI values. These Sub Cells correspond to the Epoxy Experimental 1 and the no repair method, respectively. Sub Cell 982 already consisted of diamond grinding on both lanes because it received no repairs. Since the repaired sub cells only experienced diamond grinding on the driving lanes, it made sense that the sub cell experiencing no repair method would excel in ride quality in comparison to the sub cells experiencing a repair method for the passing lane.

Since the repaired sub-cells only underwent diamond grinding on the driving lanes, it made sense that the sub-cell with no repair method would excel in ride quality compared to the sub-cells subjected to a repair method for the passing lane. The driving lane IRI data provides the most accurate comparison of the ride quality for sub cells involved in this experiment.

3.7.2 Analyses of Load Transfer Efficiency

From Figure 3.13 and Figure 3.21, the approach and leave LTE values followed very similar trends. For simplification, the graphs were separated with respect to the type of dowel repair method used for each sub cell; the different types of adhesive methods and dowel repair were in reference to the image depicted in Figure 2.3. These figures directly compared each dowel repair method when using the two different diameter steel dowels used in this experiment: 1” and 1.25”.

Overall, the results showed that the repair methods with 1.25-inch diameter steel dowels provided similar or slightly better LTE values than the same repair methods with 1 inch diameter dowels. The only repair method analyzed that indicated otherwise was the grout – capsule method; although, the difference between the LTE values of the 1” and 1.25” diameter dowels for the grout – capsule method was miniscule. These figures also showed that each repair method significantly increased the LTE from the 8/13/2013 installation date and the 9/13/2013 field test. The one sub cell that experienced no dowel rehabilitation, shown in Figure 3.19, did not produce the same spike in LTE as the other sub cells. The results indicated that any dowel rehabilitation method provided a significant improvement in LTE directly after installation.

Overall, each dowel repair method analyzed in this experiment positively affected the LTE values directly after installation. However, a few methods maintained exceptional LTE values while others significantly decreased in LTE for the following field test date (almost a year later). These results indicated which dowel repair method will likely provide long term improvements in LTE. Figure 3.28 shows the sub cells that have maintained sustainable LTE values. Figure 3.29 shows the sub cells that provided poor LTE values.

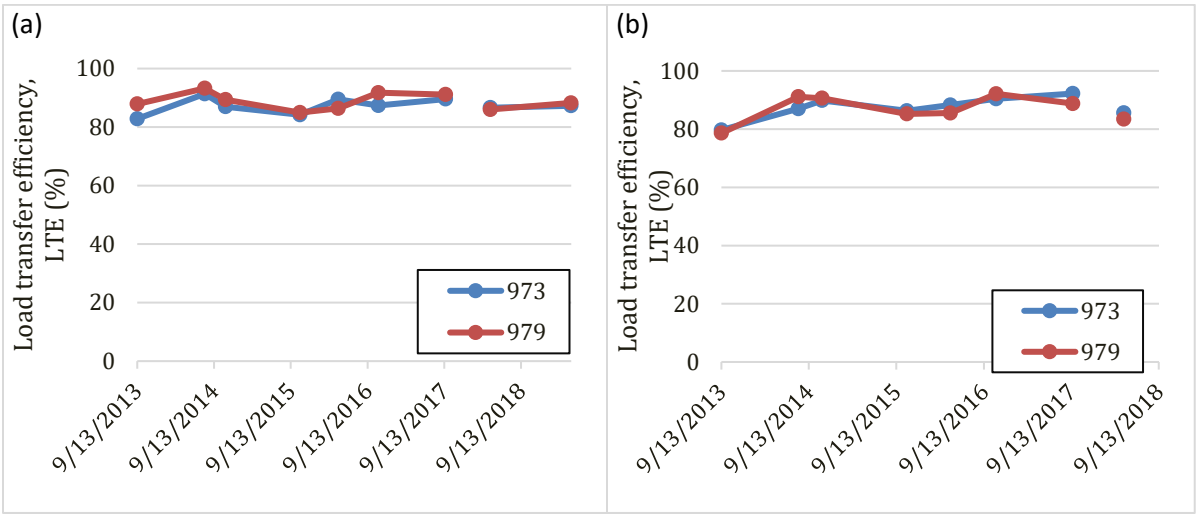

Figure 3.28 General time trend for load transfer efficiency (LTE) for top performing sub: (a) approach and (b) leave.

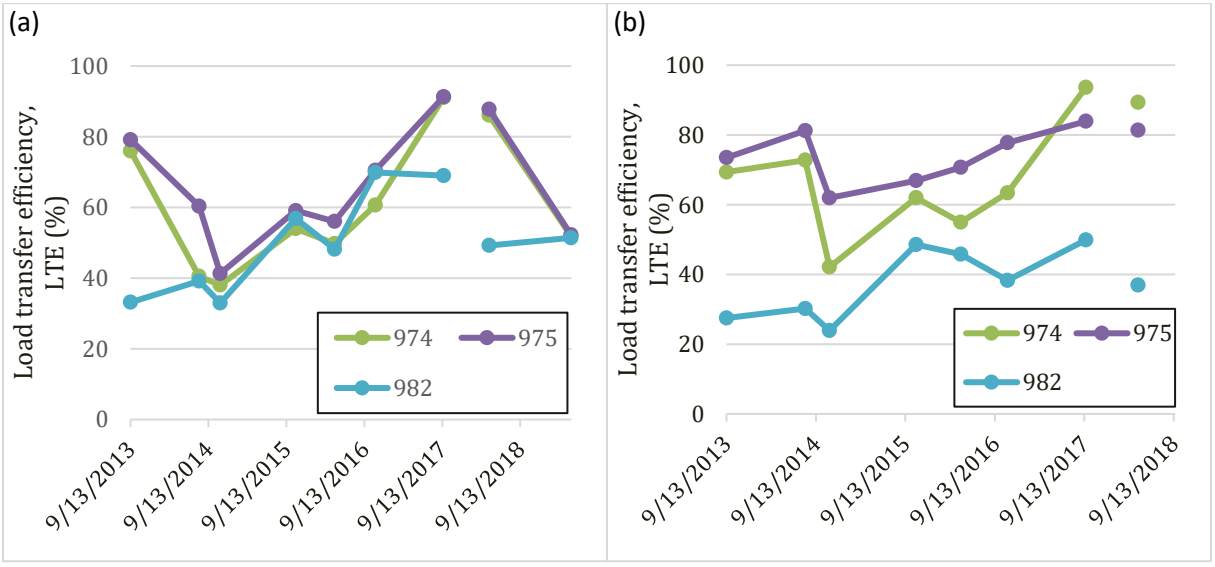

Figure 3.29 General time trend for load transfer efficiency (LTE) for poor performing sub cells: (a) approach and (b) leave.

From Figure 3.28, the grout – dip adhesive method performed similarly to the dowel repair method using no grout, suggesting that the grout – dip method was essentially a waste of grout.

The most significant, common trend within Figures 3.28 and 3.29 was that the majority of the sub cells produced an increase in LTE from spring 2016 to fall 2016. This can likely be attributed to the assumption that the base was at its weakest during the spring months due to the spring freeze thaw and

moisture content. However, two sub cells did not follow this trend; Sub Cells 970 and 971. The anchoring materials utilized in the other sub cells might have provide additional support for the steel dowels. Sub Cells 970 and 971 may have experienced a decrease from spring to fall due to the absence of adhesive in the dowel repair process. This suggests that the weakening of the steel dowels could potentially account for the decline in LTE.

Aside from the season and recent weather patterns of the field test date, these LTE trends were associated to the developing and weakening of the various forces within the joint over time. The forces within the joint included the force applied from the steel dowels, the force applied from the base below the panels, and the force applied due to the aggregate interlock. The development or weakening of these forces may vary in both time and intensity across different joints, which could explain the subtle differences observed in the trends for these test sub cells.

Following Figure 3.20 and Figure 3.21, recommendations were made to what adhesive method for dowel repair provides optimal, sustainable LTE. From Figure 3.28 and Figure 3.29 Sub Cells 973 and Cell 979 were the top performing sub cells for both approach and leave LTE values. These sub cells correspond to the grout – bag injected method with 1.25" dowels and Epoxy Experimental 2 with 1.25" dowels, respectively.

While Figure 3.28 highlighted that the grout – bag injected method and the Epoxy Experimental 2 provide the best LTE values, overall results showed that the grout – capsule method and the Epoxy Experimental 1 also provided quality, sustainable LTE values. From the figures, utilizing any of these four adhesive methods for dowel repair would provide optimal, sustainable load transfer ability across the joint. The LTE values still show a significant improvement from the sub cell with no repairs; however, these LTE values were low. When attempting to achieve optimal LTE in dowel bar repairs, the no grout method, and the grout – dip method should be avoided.

3.7.3 Traffic Implication of FWD and Ride

From Table 3.2, 2016 had the most traffic days, and 2013 had the least amount of traffic days. It is difficult to draw conclusions when comparing this traffic data to the ride quality data on these test sub cells because of the lack of data collected for the ride quality. Since there was not enough ride quality data to generate a definitive IRI time trend for these test sub cells, the IRI cannot yet be related to this traffic data.

When comparing this traffic data to the LTE data, there can potentially be some correlations made because of the larger distribution of field test dates. However, the trends of LTE data were attributed to other independent factors. When attempting to compare the LTE data to the traffic data, only the driving lane was analyzed. In addition, only fall field test dates were considered to make sure that the seasonal changes would not interfere with this comparison. When analyzing the trends in traffic data with the trends in the fall LTE data, there appeared to be no relationship between the two. This result suggests that the primary factor affecting LTE data is the seasonal changes and the internal forces strengthening and weakening within the joint.

3.7.4 Analysis of Visual Results

The results from the cores displayed in Figure 3.23 andFigure 3.24 are summarized in Table 3.4. Table 3.4 examined the quality of each sub cell in three categories: Good, Marginal, and Bad. The three Cells marked as Bad were 974, 975, and 982. These were the sub cells treated with the dip method of grout and the control Cell. The Dip Method likely does not place enough grout in the dowel hole to hold the dowel center and this unevenness may result in a breakdown of the concrete. The results from Table 3.3 were used to create Table 3.4 through Table 3.6, in which the sub cells were organized by their quality measure as well as dowel size, bonding material, and overall method. When separated by dowel size, as in Table 3.4, the smaller 1" dowel had more Good quality Cells than the larger 1.25" dowel. This difference might be because as dowel diameter or length increases, so does strength of the dowel, and by comparison, the surrounding concrete is weaker and more likely to breakdown as traffic causes small shifts in the dowel.

When separated by bonding material, Epoxy bonding material constituted more good quality performance compared to the grout and no bonding material cell. In Table 3.6 these categories are separated further into the overall techniques used for each Cell. While epoxy in general appeared to do better than grout, the Epoxy Experimental 1 appeared to do better than the Epoxy Experimental 2, further investigation of the materials used in these epoxies would be needed to understand why this was the case. Again, when considering the Bad category, the Dip Method and control performed worst. The control was not repaired, rather the dowel located in the core had been in the sub cell for 40 years. The rust is likely due to age, while unlikely to be a design flaw it is worth noting that rust around a dowel will weaken the concrete-pavement interface that will generally lead to the dowel hole increasing in size vertically from concrete erosion or transverse cracking as displayed in the core of Sub Cell 982 the control where no repair was done.

3.7.5 Analysis of Faulting Results

Although there is huge variability in the disparity between the faulting of the 1.25 inch and the 1-inch dowel in each of the repair methods, it was evident that there is in a general trend, the faulting being larger in the larger diameter dowel. In Figure 3.26 a direct comparison of faulting done between 1' diameter and corresponding test sections with 1.25 ' diameter dowels. Results are also accentuated by Table 3.7 and Table 3.8. In Table 3.7 descriptive statistics showed low mean faulting in the lower diameter dowels. Relative distributions are shown in Figure 3.27. A t-test shows that the two data sets are dissimilar based on an alpha value of 0.05.

A repeatable measurement of 1/8th of an inch is the threshold for realistic faulting distress. The distribution shows the 1/8th of an inch as the 85-percentile value in the 1' diameter dowel sections and 80-percentile on the larger diameter dowel sections. One explanation that would have been proffered is the sufficiency of the anchorage material around the dowels. The argument would have been based on the fact that the drilled holes were of the same diameter and resulted in a thinner annular space and in consequence a smaller filling between the dowel and pavement. If that was tenable then why was this

anomaly still evident in the no grout segments 970 and 971? Another explanation was based on the actual effect of dowel diameter. It is evident and obvious from the preceding arguments that the major distinguishing factor is the dowel. The larger diameter may be a source of stress concentrations to the dowels. Especially as the anchorage material makes the dowel behave as an anchorage on one end and as a dowel on the other end.

Chapter 4: Conclusions and Recommendations

4.1 Conclusions

The ride quality (IRI) and joint load transfer (LTE) results indicated significant similarities among the performance of the various adhesive methods analyzed for the dowel repairs. For both the IRI and LTE, the same four adhesive methods provided quality data, proving to be ideal candidates to be considered for use in dowel repairs. The four adhesive methods that would likely provide optimal, sustainable load transfer ability and ride quality when performing dowel repairs were grout — bag injected, grout — capsule, Epoxy Experimental 2, and Epoxy Experimental 1. The data also showed that two adhesive methods performed poorly for both load transfer ability and ride quality. The poorly performing materials and methods in comparison to the others included the method using no grout for repairs and the grout–dip method.

While the results from the IRI data mostly align with the results from the LTE data, the lesser amount of ride quality data caused the analysis to rely more on distress survey analysis. Therefore, the LTE data was more reliable. There were also too many external factors that could have an effect on the overall measured ride quality of these sub cells. These repairs occurred at the joints within each sub cell, and the IRI data accounted for the ride quality of the entire sub cell, meaning that the ride quality was not necessarily reflective of the performance of the adhesive methods investigated in this study. The LTE data was more indicative of the advantages and disadvantages of each adhesive method used in this dowel repair experiment due to the plethora of field test dates. LTE was also the primary factor that was affected by this experiment since these repairs occurred at the joints.

When trying to determine the dowel rehabilitation methods that produced the optimal LTE values, it was evident that Sub Cells 973 and 979 provided the most sustainable results. The difference between the LTE results of these two top-performing sub cells were minor; however, it was determined that test Sub Cell 973 provided the most optimal LTE values over time. Test Sub Cell 973 corresponded to the grout-bag injected method with 1.25-inch steel dowels. Ultimately, using any of the adhesive methods for dowel repairs analyzed in this study produced sufficient load transfer ability with the exception of the no-grout method and the grout–dip method.

The grout-dip method proved to underperform in the primary experiment discussed in this report, which supports the results of the previously performed in-house experiment. These results reinforced the conclusion that using the grout–dip method will provide inadequate results when implementing dowel repairs.

Research concluded that based on pavement smoothness, load transfer and visuals the epoxy and grout-filled sub cells performed better than those without grout or epoxy and much better than the unrepaired portion. However, the Epoxy Experimental 1 appeared to be the best performing material. The 1-inch diameter appeared to perform better than the 1.25-inch diameter dowel in this experiment.

The unrepaired sub cell showed a plane of delamination tangential to the dowel. This plane appeared to be a logical stress relief mechanism in reaction to the bearing stresses occurring in a distressed anchorage system. It appeared that socketing would continue to occur if there were no plane of delamination. The factor that selectively resulted in socketing versus plane of delamination was a fracture mechanics issue beyond the level of this report.

4.2 Recommendations

Evidently, these results validated the in-house experiment in which the epoxy-based methods generally presented better performance than the grouts, but all appear to be within the bounds of marginal to good performance. In terms of IRI, LTE, and visual observation, the poor performing cells were clearly those without epoxy and without repair. It appeared that if due diligence were to be done in mixing and placing dowels, irrespective of the material type or product, there would be a high probability that it would meet the criteria for good performance.

The experiment demonstrated that care must be taken in the choice of dowel diameter. Since in most of the cases, sections with larger dowels performed worse than those with smaller-sized dowels, it means that larger dowels than necessary will induce counterproductive bearing stresses.

This experiment did not explore the suitability of a lesser number of dowels per cross section in a repair, as in all cases, there were 11 dowels across each panel.

References

[1] Burnham, T., & Izevbekhai, B. (2009). Retrofit dowel bars in jointed concrete pavement—Long-term performance and best practices. Paper presented at the National Conference on Preservation, Repair, and Rehabilitation of Concrete Pavements, St. Louis, MO, April 22–29.

[2] National Concrete Pavement Technology Center. (2011). *Guide to dowel load transfer systems for jointed concrete roadway Pavements*. Ames, IA: Iowa State University.

[3] Izevbekhai, B. I., Van Deusen, D. A. (2015). Forensic evaluation of multiple cracking of a concrete test Cell built over an open graded aggregate base. *International Journal of Forensic Engineering, 2*(3), 189–208.

[4] Embacher, E. (2001). *Construction report on the installation of retrofit dowel bar rest sections on TH 23* (No. MN/RC-2001-0). St. Paul, MN: MnDOT.